

**IZMIR KATIP CELEBI UNIVERSITY
GRADUATE SCHOOL OF NATURAL AND APPLIED SCIENCES**

**COMPACT RECTENNA DESIGN
FOR
RF ENERGY HARVESTING APPLICATIONS**

M.Sc. THESIS

Cem GÖÇEN

Department Of Electrical And Electronics Engineering

Thesis Advisor: Assoc. Prof. Dr. Merih PALANDÖKEN

JUNE 2019

IZMIR KATIP CELEBI UNIVERSITY
GRADUATE SCHOOL OF NATURAL AND APPLIED SCIENCES

COMPACT RECTENNA DESIGN
FOR
RF ENERGY HARVESTING APPLICATIONS

M.Sc. THESIS

Cem GÖÇEN
Y160207011

Department Of Electrical And Electronics Engineering

Thesis Advisor: Assoc. Prof. Dr. Merih PALANDÖKEN

JUNE 2019

İZMİR KATİP ÇELEBİ ÜNİVERSİTESİ
FEN BİLİMLERİ ENSTİTÜSÜ

RF ENERJİ HASATLAMA UYGULAMALARI
İÇİN
KOMPAKT DOĞRULTUCULU ANTEN (RECTENNA) TASARIMI

YÜKSEK LİSANS TEZİ

Cem GÖÇEN
Y160207011

Elektrik Elektronik Mühendisliği Ana Bilim Dalı

Tez Danışmanı: Doç. Dr. Merih PALANDÖKEN

HAZİRAN 2019

Cem GÖÇEN, a M.Sc. student of **Izmir Katip Çelebi University Graduate School Of Natural And Applied Sciences**, successfully defended the thesis entitled “**COMPACT RECTENNA DESIGN FOR RF ENERGY HARVESTING APPLICATIONS**”, which he prepared after fulfilling the requirements specified in the associated legislations, before the jury whose signatures are below.

Thesis Advisor :

Assoc. Prof. Dr. Merih PALANDÖKEN
Izmir Katip Çelebi University

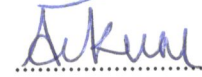


Jury Members :

Assoc. Prof. Dr. Merih PALANDÖKEN
Izmir Katip Çelebi University



Prof. Dr. Adnan KAYA
Izmir Katip Çelebi University



Prof. Dr. Mustafa SEÇMEN
Yaşar University



Date of Submission : 20.06.2019
Date of Defense : 17.06.2019

THE UNIVERSITY OF CHICAGO
DEPARTMENT OF CHEMISTRY
5408 SOUTH DICKENS STREET
CHICAGO, ILLINOIS 60637

11/10/1964

Dear Mr. [Name]

11/10/1964

11/10/1964

11/10/1964

Dear Mr. [Name]

THE UNIVERSITY OF CHICAGO
DEPARTMENT OF CHEMISTRY

To my family,

FOREWORD

First and foremost, I would like to thank my advisor, Assoc. Prof. Dr. Merih Palandöken, for support and guidance throughout my study. It was an honor me to work with a very successful and knowledgeable advisor in your work. Also, I would like to thank you very much for your guidance as a younger brother both in my study and others.

I would like to express my gratitude to the head of our department, my thesis jury, Prof. Dr. Adnan Kaya, for giving every opportunity for the success of the study as well as providing me a scholarship in your Tubitak project. I would also like to thank my colleagues Res. Asst. Cem Baytöre, Res. Asst. İsmail Akdağ, and Caner Murat for their support and assistance in my studies.

My heartiest thanks and most profound appreciation is due to my parents, my sister and my fiancée, Hatice Küçükönder M.D., for standing beside me, encouraging and supporting me all the time I have been working on this study.

Thanks to all those who assisted me in all terms and helped me to bring out this study.

This thesis was supported by the research projects of Izmir Katip Çelebi University, BAP (Scientific Research Coordination Office of Scientific Research Projects) under the project grant no: 2018-TYL-FEBE-0058, TURKEY.

June 2019

Cem GÖÇEN

TABLE OF CONTENTS

	<u>Page</u>
FOREWORD	ix
TABLE OF CONTENTS	xi
ABBREVIATIONS	xiii
LIST OF TABLES	xv
LIST OF FIGURES	xvii
ABSTRACT	xxi
ÖZET	xxiii
1. INTRODUCTION	1
1.1 Introduction	1
1.2 Motivation	2
1.3 Aim and Objectives	3
1.4 Contributions	3
1.5 Thesis Overview	4
2. RADIO FREQUENCY ENERGY HARVESTING	5
2.1 Radio Frequency Energy Harvesting System Overview	6
2.2 Literature Review of RF Energy Harvesting.....	8
2.3 Ambient RF Energy Sources	15
2.4 Antenna	17
2.4.1 Antenna parameters.....	17
2.5 Impedance Matching Circuit	22
2.6 Rectifying Circuit	24
2.7 DC Load	29
2.8 RF Energy Harvesting System Efficiency	30
3. RF ENERGY HARVESTING SYSTEM DESIGN CONSIDERATIONS	31
3.1 RF Survey.....	34
3.2 Rectenna Design – 1	35
3.2.1 Energy harvesting antenna design.....	35
3.2.2 Impedance matching and RF to DC rectifying circuit design.....	37
3.3 Rectenna Design – 2.....	39
3.3.1 Energy harvesting antenna design.....	39
3.3.2 Impedance matching and RF to DC rectifying circuit design.....	41
4. NUMERICAL AND EXPERIMENTAL RESULTS	43
4.1 Rectenna Design – 1	43
4.2 Rectenna Design – 2.....	54
5. CONCLUSION AND FUTURE WORK	65
5.1 Conclusion.....	65
5.2 Future Work	66
REFERENCES	67
CURRICULUM VITAE	75

ABBREVIATIONS

2D	: Two Dimensional
3D	: Three Dimensional
3G	: Third Generation
4G	: Fourth Generation
AC	: Alternate Current
AF	: Antenna Factor
AM	: Amplitude Modulation
BW	: Bandwidth
CST	: Computer Simulation Technology
CMOS	: Complementary Metal-Oxide Semiconductor
dB	: Decibel
dB_i	: Decibel Isotropic
DC	: Direct Current
EM	: Electromagnetic
FM	: Frequency Modulation
IEEE	: Institute of Electrical and Electronics Engineers
ISM	: Industrial Scientific and Medical Band
GHz	: Gigahertz
GPS	: Global Positioning System
GSM	: Global System for Mobile Communications
Hz	: Hertz (cycles per second)
IC	: Integrated Circuit
LAN	: Local Area Network
LTE	: Long Term Evolution
MHz	: Megahertz
PCB	: Printed Circuit Board
RF	: Radio Frequency
RFID	: Radio Frequency Identification
SHF	: Super High Frequency
SMA	: Sub-miniature A
SMT	: Surface Mount Technology
SMD	: Surface Mount Device
UHF	: Ultra High Frequency
UMTS	: Universal Mobile Telecommunications System
VHF	: Very High Frequency
WiFi	: Wireless Fidelity
WiMAX	: Worldwide Interoperability for Microwave Access
WLAN	: Wireless Local Area Network
WPT	: Wireless Power Transfer
WSN	: Wireless Sensor Network

LIST OF TABLES

	<u>Page</u>
Table 2.1 : Estimated power values from different energy harvesting techniques [2].	5
Table 2.2 : Comparison of different wireless energy transfer techniques [3;5;6].....	8
Table 3.1 : Literature review of RF energy harvesting systems operating at 900 MHz.	32
Table 3.2 : Literature review of RF energy harvesting systems operating at 2.4 GHz.	33
Table 3.3 : Skyworks SMS 7630 Spice parameters.	38
Table 3.4 : Design parameters of proposed impedance matching and RF to DC rectifying circuit with DC load.	38
Table 3.5 : Design parameters of proposed impedance matching and RF to DC rectifying circuit with DC load.	42
Table 4.1 : Rectenna Design – 1 simulated performance parameters.	53
Table 4.2 : Rectenna Design – 2 simulated performance parameters.	64

LIST OF FIGURES

	<u>Page</u>
Figure 2.1 : RF energy harvesting system block diagram.....	6
Figure 2.2 : Different antenna designs used for RF energy harvesting; (a) probe-fed microstrip patch antenna [26], (b) 50 Ω folded dipole antennas [27], (c) flexible yagi antenna [28], (d) small loop antenna [29], (e) anti-spiral slot resonator antenna [30], and (f) circular patch array antenna [31].....	9
Figure 2.3 : Radio frequency spectrum [56].	15
Figure 2.4 : The path loss in dB with increasing distance at 900 MHz and 2.4 GHz.	17
Figure 2.5 : Antenna field regions [57]......	18
Figure 2.6 : Antenna polarization types [60].	21
Figure 2.7 : Antenna equivalent model.	22
Figure 2.8 : Matching network between the antenna and the rectifying circuit.....	23
Figure 2.9 : Half-wave rectifier.....	25
Figure 2.10 : Full-wave rectifier.	25
Figure 2.11 : Equivalent circuit of a Schottky diode [67].....	26
Figure 2.12 : Single stage Villard voltage doubler circuit.	27
Figure 2.13 : Different voltage rectifier topologies: (a) 2-stage Villard voltage rectifier, (b) 2-stage Greinacher voltage rectifier, and (c) 2-stage Dickson voltage rectifier.	28
Figure 2.14 : N-Stage voltage rectifier.....	29
Figure 2.15 : RF energy harvesting system with DC load resistance.	30
Figure 3.1 : RF signal measurement devices: (a) Survey meter, (b) Personnel dosimeter, and (c) Spectrum analyzer.	34
Figure 3.2 : (a) top and (b) bottom surfaces of energy harvesting antenna model with design parameters (The relevant dimensions are (in mm); R1=18, R2=20, R3=22, R4=24, D1=2.5, D2=2, L1=81.25, L2=87.5, L3=23, L4=8.2, L5=30.1, L6=34.375, L7=12.5, M1=43.75, M2=40.625, Rg1=32.5, Rg2=27.5, Rg3=5, Rg4=6.5, ● is feeding point), (c) top, and (d) bottom views of the fabricated prototype of energy harvesting antenna design.....	36
Figure 3.3 : (a) Configuration of the proposed RF energy harvesting system (antenna, matching circuit, rectifying circuit, and DC load), (b) matching circuit (c) Villard voltage rectifier circuit, and (d) DC load (temperature sensor).	37
Figure 3.4 : (a) top and (b) bottom layers of energy harvesting antenna model with design parameters (The relevant dimensions are (in mm); H1=41.8, H2=22, C1=1.9, C2=13.4, C3=1.7, C4=8.8, C5=4.6, C6=2.7, C7=4, C8=13.5, C9=1.5, C10=12.8, C11=3.2, C12=2, G1=8.3, G2=21, G3=25.2, G4=0.5, and ● are feeding points), (c) top, and (d) bottom views of the fabricated prototype of energy harvesting antenna design.	40

Figure 3.5 : (a) Configuration of the proposed RF energy harvesting system (antenna, matching circuit, rectifying circuit, and DC load), (b) matching element (circuit) (c) Villard voltage rectifier circuit, and (d) DC load.	41
Figure 4.1 : The input reflection coefficient (S_{11}) of the modeled in CST and fabricated energy harvesting antenna.	43
Figure 4.2 : The input reflection coefficient (S_{11}) of the proposed energy harvesting antenna with the different variables; (a) R_{g1} is variable (others are constant) and (b) R_{g2} is variable (others are constant).	45
Figure 4.3 : The surface current distributions of the energy harvesting antenna at the resonance frequency; (a) top and (b) bottom views.	46
Figure 4.4 : The 2D (polar plot) radiation patterns of the energy harvesting antenna at the resonance frequency 900 MHz: (a) antenna design with coordinate system for demonstration of planes (b) X-Y plane, (c) X-Z plane, and (d) Y-Z plane..	47
Figure 4.5 : The 3D radiation pattern of the proposed energy harvesting antenna at the resonance frequency of 900 MHz.	48
Figure 4.6 : RF energy harvesting antenna input power measurement setup.	48
Figure 4.7 : Terminal (a) voltage and (b) current values on the lumped element (antenna feeding port).	49
Figure 4.8 : The input reflection coefficient of the RF energy harvesting system at the resonance frequency with different RF input values.	50
Figure 4.9 : The RF to DC conversion efficiency of the impedance matching and RF to DC rectifying circuit at the resonance frequency with different RF input values.	51
Figure 4.10 : The output DC voltage values of the impedance matching and RF to DC rectifying circuit at the resonance frequency with different RF input values.	51
Figure 4.11 : The DC output voltage level of the impedance matching and RF to DC rectifying circuit at the resonance frequency with different DC load resistance.	52
Figure 4.12 : RF input and output DC voltage values of the proposed impedance matching and RF to DC rectifying circuit for -11 dBm input RF power.	53
Figure 4.13 : The input reflection coefficient (S_{11}) of the modeled in CST and fabricated energy harvesting antenna.	54
Figure 4.14 : The input reflection coefficient (S_{11}) of the proposed energy harvesting antenna with the different variables; (a) G_4 parameter is variable (others are constant), and (b) C_2 parameter is variable (others are constant).	55
Figure 4.15 : The surface current distribution of the proposed energy harvesting antenna; (a) top and (b) bottom layers.	56
Figure 4.16 : The 2D (polar plot) radiation patterns of the energy harvesting antenna at the resonance frequency 2.4 GHz: (a) antenna design with coordinate system for demonstration of planes (b) X-Y plane, (c) X-Z plane, and (d) Y-Z plane..	57
Figure 4.17 : The 3D radiation pattern of the proposed energy harvesting antenna at the resonance frequency of 2.4 GHz.	58
Figure 4.18 : Energy harvesting antenna input power measurement setup.	58
Figure 4.19 : (a) Voltage and (b) current values on the lumped element (antenna feeding port).	59
Figure 4.20 : The input reflection coefficient of the RF energy harvesting system at the resonance frequency with different RF input values.	60

Figure 4.21 : The RF to DC conversion efficiency of the impedance matching and RF to DC rectifying circuit at the resonance frequency with different RF input values.....	61
Figure 4.22 : The output DC voltage values of the impedance matching and RF to DC rectifying circuit at the resonance frequency with different RF input values.	62
Figure 4.23 : The DC output voltage level of the impedance matching and RF to DC rectifying circuit at the resonance frequency with different DC load resistance.	62
Figure 4.24 : The RF to DC conversion efficiency of the impedance matching and RF to DC rectifying circuit at the resonance frequency with different DC load resistance.	63
Figure 4.25 : RF input and output DC voltage values of the proposed impedance matching and RF to DC rectifying circuit for -11dBm input RF power (V_{in} – Input RF signal (from the antenna), V_{in1} – RF to DC rectifying circuit input signal (after matching), and V_{out} – Output DC voltage).....	64

COMPACT RECTENNA DESIGN FOR RF ENERGY HARVESTING APPLICATIONS

ABSTRACT

In this study, a detailed literature study has been conducted about radio frequency energy harvesting systems, and two different RF energy harvesting system designs are presented operated two different bands. RF energy harvesting systems have been in our lives for more than fifty years. The number of studies carried out on these systems has increased, especially to meet the power requirements of low power consumption devices whose usage is growing with the developing technology in recent years. In the literature, RF energy harvesting systems have been generally designed to operate in the ultra-high-frequency band. For this purpose, two different RF energy harvesting systems operating in this frequency band have been developed. While determining the operating frequencies of the proposed systems, GSM and ISM bands widely used have been preferred. The RF energy harvesting system consists of a receiving antenna, a rectifier circuit that converts RF signals into DC signals, and an impedance matching circuit between the antenna and rectifier circuit.

Antennas have been designed, numerically calculated in CST Studio Suite using the Rogers RO4003 substrate, and verified by the fabricated prototype. RF to DC rectifying and impedance matching circuits have been designed and numerically calculated as a nonlinear in Ansoft Designer and Ansys Electronics Desktop. The proposed system designs have achieved successful performance parameters: The system design operating at 900 MHz has been yielded 1.7 V DC output voltage with 75 % RF-DC conversion efficiency at -11 dBm input power. The system design operating at 2.4 GHz has been generated 0.75 V DC output voltage with 49 % RF-DC conversion efficiency at -11 dBm input power. As a result, essential information about RF energy harvesting systems has been presented, and successful performance parameters have been obtained in the designed systems. Also, suggestions on increasing output DC voltage are presented in this study.

RF ENERJİ HASATLAMA UYGULAMALARI İÇİN KOMPAKT DOĞRULTUCULU ANTEN (RECTENNA) TASARIMI

ÖZET

Bu çalışmada, radyo frekans enerji toplama sistemleri hakkında detaylı bir literatür çalışması gerçekleştirilmiş ve iki farklı bantta çalışmak üzere tasarlanan iki farklı RF enerji toplama sistemi tasarımı sunulmuştur. RF enerji hasatlama sistemleri elli yıldan uzun bir süredir hayatımızda yer almaktadır. Bu sistemler ile ilgili yürütülen çalışmaların sayısı özellikle son yıllarda gelişen teknoloji ile birlikte kullanımı artan düşük güç tüketimi olan cihazların güç ihtiyacını karşılamak amacıyla artmıştır. Literatürde bulunan RF enerji hasatlama sistem tasarımları genellikle ultra yüksek frekans bandında çalışmaktadır. Bu amaçla bu frekans bandında çalışan iki adet farklı RF enerji hasatlama sistem tasarımı oluşturulmuştur. Önerilen sistemlerin çalışma frekansları belirlenirken ise kullanımları oldukça yaygın olan GSM ve ISM bantları tercih edilmiştir. RF enerji hasatlama sistemi alıcı anten, RF sinyalleri DC sinyallere dönüştüren doğrultucu devre ve anten ile doğrultucu devre arasında bulunan empedans eşleştirme devresinden oluşmaktadır.

Anten tasarımları Rogers RO4003 alttaş malzemesi kullanılarak CST Studio Suite programında tasarlanmış, nümerik olarak hesaplanmış ve fabrike edilen prototip ile doğrulanmıştır. RF - DC doğrultucu devre tasarımları ile empedans eşleştirme devresi ile birlikte Ansoft Designer ve Ansys Electronics Desktop programlarında nonlineer olarak tasarlanmış ve nümerik olarak hesaplanmıştır. Önerilen sistem tasarımları başarılı sonuçlara ulaşmıştır: 900 MHz de çalışan sistem tasarımı ile -11 dBm giriş gücünde % 75 RF-DC dönüşüm verimiyle 1.7 V DC çıkış voltajı elde edilmiştir. 2.4 GHz de çalışan sistem tasarımı ile -11 dBm giriş gücünde % 49 RF-DC dönüşüm verimiyle 0.75 V DC çıkış voltajı elde edilmiştir. Sonuç olarak, yürütülen çalışmada RF enerji hasatlama sistemleri ile önemli bilgiler sunulmuş ve tasarımları gerçekleştirilen sistemlerde başarılı performans verileri elde edilmiştir. Ayrıca çıkış voltaj değerini arttırmak üzerine bazı öneriler de bu çalışmada sunulmuştur.

1. INTRODUCTION

1.1 Introduction

In this thesis, a study on Radio Frequency (RF) Energy Harvesting System (Rectenna) is presented. The word rectenna is a compound of “rectifier” and “antenna” The primary purpose of this study is to analyze the feasibility of using RF energy harvesting to power an electronic device that is in general low power consumption by using ambient radio frequency sources in the environment and providing appropriate system design.

Electronic devices are an undetachable part of our lives, and with the developing technology, this part gets increased. The increasing use of wireless devices has led to increased demand and supply in need of batteries to be more efficient. Using disposable/ rechargeable batteries as the source of energy impose of wireless devices several limitations, including the need for maintenance of batteries and cost involved in replacing batteries. Also, some batteries contain heavy metals such as lead, cadmium, and mercury, which can pollute the environment if they are disposed of improperly. Due to negative aspects, batteries could be replaced by alternative sources, such as Direct Current (DC) power generators using energy harvesting techniques.

Radio frequency energy harvesting is defined as the process of extracting energy from the surroundings of a system and converting it into usable DC signal for any electronic devices [1]. In general, an energy harvesting system consists of the following components:

- An ambient energy source,
- A transducer (rectifying circuit) - converting ambient energy into electrical energy,
- An energy storage component or load - storing the harvested energy and powering the sensor system,

There are different kinds of ambient available in the environment that can be utilized for energy harvesting such as solar, thermal, vibration, wind, and radio frequency (RF) energy.

The RF energy harvesting is based on the gathering of RF signals in the RF fields generated by electromagnetic waves radiated by electromagnetic wave sources such as TV towers, wireless radio networks, and mobile phone towers. This RF signal is captured and converted into functional DC voltage by using a rectifying circuit directly connected to a receiving antenna. Electromagnetic waves are freely available at an increasing frequency and power level in the environment, especially in densely populated urban areas. RF energy sources are available in our environment and suitable for use in energy harvesting systems:

FM (Frequency Modulation) Band: 87.5 – 108 MHz

Radio Communication Band: 370 – 450 MHz

VHF (Very High Frequency) Band: 174 – 230 MHz

UHF (Ultra High Frequency) Band: 470 – 854 MHz

GSM (Global System for Mobil Communication) 900 Band:

880 – 915 MHz (uplink) mobile to base

935 – 960 MHz (downlink) base to mobile

GSM (Global System for Mobil Communication) 1800 Band:

1710 – 1785 MHz (uplink) mobile to base

1805 – 1880 MHz (downlink) base to mobile

WiFi (Wireless Fidelity) Band: 2400 – 2480 MHz

ISM (Industrial Scientific Medical) 2.4 GHz Band: 2400-2483 MHz

3G (Third Generation of Mobile Phone) Band: 2110 – 2200 MHz

WiMax (Worldwide Interoperability for Microwave Access) Band: 3400 – 3600 MHz

1.2 Motivation

People need energy, which is a fundamental need to sustain their various vital activities. The energy in nature can be converted between different forms, stored, transferred, and never eliminated. With the developing technology, there has been a

significant increase in energy resource diversity, energy storage capacity, and the conversion efficiency of energy between types. Energy supply has always been a critical limiting factor to the lifetime of some electronic devices, especially wireless devices.

The motivation behind this thesis study is that, despite the disadvantages of limited battery life and where there is difficulty in energizing, by exploring possible alternatives to conventional, disposable batteries in powering the electronic devices with low power consumption, thus making these devices indefinitely self-sustaining. One possible solution is to use radio frequency (RF) energy harvesting, in which ambient energy is gathered, converted into electrical energy, and used.

1.3 Aim and Objectives

The study presented in this thesis aims to develop rectennas (energy harvesting systems) which operates at different frequency bands for RF wireless energy harvesting.

The objectives are:

- ✓ To investigate various types of energy harvesting antennas and to improve the appropriate antenna design.
- ✓ To investigate RF to DC rectifying circuit of energy harvesting systems and to improve the appropriate circuit design.
- ✓ To achieve high RF to DC conversion efficiency as a result of the RF energy harvesting system consisting of an RF energy harvesting antenna and RF to DC rectifying circuit.

1.4 Contributions

This thesis summarizes the main contributions of the work as follows:

This study presents two different RF energy harvesting systems. One of the energy harvesting systems is designed to operate in the 900 MHz band, and the other is designed to operate in the 2.4 GHz band.

The designed energy harvesting antenna structures and rectifier circuits have been verified using various simulation programs, analyzes and performance tests have been done in these programs. It has been ensured that every fabricated element gives measurement results compatible with the simulation result, and otherwise, their causes have been investigated.

Antenna and rectifying circuit designs have been designed to operate correctly even at low power levels. The energy harvesting antennas have a broadband operation and a meager return loss value in this operating band. Rectifying circuit designs have input impedance values that can operate to match with 50 Ω line impedance.

For the RF energy harvesting system to operate in high efficiency, the antenna and rectifier circuit designs have been fabricated using low loss substrate. Also, to achieve high efficiency, zero bias Schottky diodes are used in rectifying circuit design.

1.5 Thesis Overview

This thesis is organized as follows:

- Chapter 2 gives a comprehensive review of RF energy harvesting system solutions proposed by researchers in the scientific literature. The basics of an RF energy harvesting system are discussed and reviewed.
- Chapter 3 describes the design, and fabrication of the RF energy harvesting systems consists of RF energy harvesting antenna, impedance matching, and RF to DC rectifying circuit, operate at 900 MHz and 2.4 GHz.
- Chapter 4 describes the simulation and measurement results of the RF energy harvesting systems, consists of RF energy harvesting antenna, impedance matching, and RF to DC rectifying circuit, operate at 900 MHz and 2.4 GHz.
- Chapter 5 presents conclusion remarks and future work.

2. RADIO FREQUENCY ENERGY HARVESTING

Energy harvesting is a process that generates power from energy sources in the environment. Energy harvesting from different sources has been in the focus of the research studies in recent years. Energy harvesting systems utilizing clean and renewable resources can be examined under the following headings: Solar energy harvesting, Vibrational energy harvesting, Thermal energy harvesting, Piezoelectric energy harvesting, and RF energy harvesting. Also, the estimated harvested power values of these energy harvesting techniques are presented in Table 2.1.

Table 2.1 : Estimated power values from different energy harvesting techniques [2].

Energy Source	Harvesting Technique	Estimated Harvested Power
Sun (outside)	Solar energy harvesting	$10^4 \mu\text{W}/\text{cm}^3$
Thermal gradient	Thermal energy harvesting	$10^1 \mu\text{W}/\text{cm}^3$
Piezoelectric	Piezoelectric energy harvesting	$5 \times 10^2 \mu\text{W}/\text{cm}^3$
RF	Radio Frequency energy harvesting	$10^1 \mu\text{W}/\text{cm}^3$

Solar energy can be turned into electrical energy using a solar cell. The solar energy harvesting technique is the most promising candidate for energy harvesting as it has the highest energy density among the energy harvesting options and it has commercially available solar cells which can be produced in various sizes.

Thermal energy harvesting is a technique developed using natural temperature variations in the environment. The thermoelectric generator is used to convert thermal energy into electrical energy.

Piezoelectric energy harvesting is a technique that converts oscillating mechanical energy into electrical energy using piezoelectric materials.

Radio frequency energy harvesting is a technique that harvests energy by gathers radio frequency signals in the environment. In this harvesting technique, ambient RF signals are gathered through the antenna and converted into electrical energy by rectifying circuit. Although the harvested power level was low, this technique attracted the attention of many researchers, and various studies were carried out in this field.

2.1 Radio Frequency Energy Harvesting System Overview

Radio frequency (RF) energy harvesting is a system that targets gathering energy that is freely available in the environment from external ambient RF sources for providing energy to the low power electronic devices. In this study, ‘Radio frequency’ (‘RF’) refers to electromagnetic waves with frequencies in the range from 3 kHz to 300 GHz. The amount of energy to be harvested can be in macro scale or micro scale for the RF energy harvesting system [3]. In general, an RF energy harvesting system consists of the following components: Ambient RF energy source(s), receiving (energy harvesting) antenna, matching circuit, RF-DC rectifying circuit, and DC load. The basic RF energy harvesting system block diagram shown in Figure 2.1.

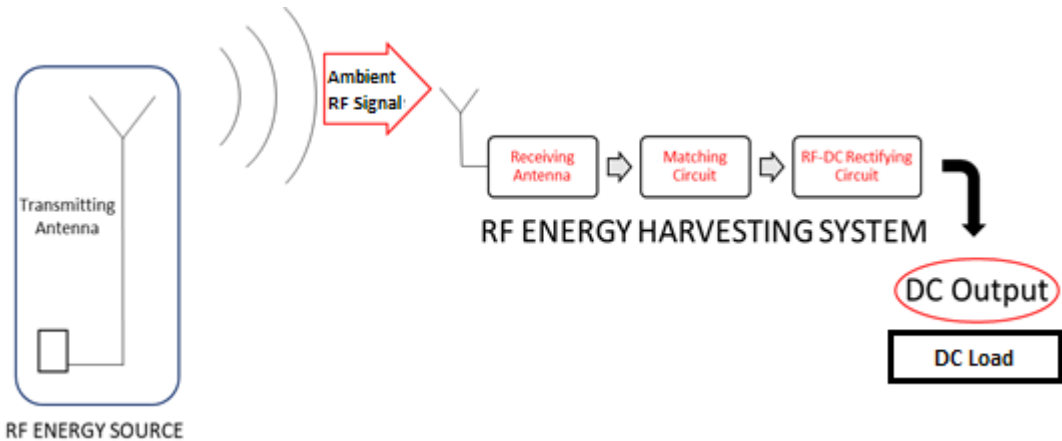


Figure 2.1 : RF energy harvesting system block diagram.

A radio frequency energy harvesting system (rectenna-rectifying antenna) consists of two main subsystems, receiving antenna and RF-DC rectifying circuit. An RF energy source is responsible for generating and radiating RF signals into the environment. The

receiving antenna used to gather RF signals which are radiated from the RF source and freely available on the environment. The RF-DC rectifying circuit converts the RF signals gathered by the receiving antenna into a DC output voltage with a high RF-DC conversion efficiency ratio. If there is an impedance mismatch between the output port of the receiving antenna and the input port of the RF-DC rectifying circuit, a matching circuit is used to increase the efficiency of the energy harvesting system by minimizing the return losses.

Wireless energy transfer is in the headpiece of the RF energy harvesting system. The wireless energy transfer topic includes inductive coupling, magnetic resonance coupling, and electromagnetic radiation. Inductive coupling and magnetic resonance coupling applications are highly efficient techniques, but it is limited by difficulties in application to the near-field of the RF source accommodates. RF energy transfer (harvesting) system is the application of electromagnetic radiation and study implement in the far-field of the RF source. Wireless power transfer techniques are summarized in Table 2.2.

The amount of harvesting power depends on the average power density of the location, efficiency of power conversion (RF to DC), and size of the energy harvesting system. The performance of the RF energy harvesting system depends on the efficiency of the rectenna, which can be improved by the antenna design, impedance matching, and modeling of the diode [4].

Table 2.2 : Comparison of different wireless energy transfer techniques [3;5;6].

Wireless Energy Transfer Technique	Operating Area	Efficiency	Applications
Resonant Inductive Coupling	Near-field (Non-radiative propagation)	From 5.81 % to 57.2 % when frequency varies from 16.2 kHz to 508 kHz	Contactless smart cards, cell phone charging
Magnetic Resonance Coupling	Near-field (Non-radiative propagation)	From the above 90 % to above 30 % when distance varies from 0.75 m to 2.25 m	PHEV charging, cell phone charging
RF Energy Transfer	Far-field (Radiative propagation)	Depends on the input power. 0.4 % at -40 dBm, above 18.2 % at -20 dBm and above 50 % at -5 dBm	Wireless sensor network, wireless body network

2.2 Literature Review of RF Energy Harvesting

RF energy harvesting systems are often used for two different purposes, to meet the energy needs of low power consumption device [7–11] and storage of the harvested energy in the storage unit (device) [12–15]. Also, RF energy harvesting systems have been used in microwave energy harvesting for space solar power satellite applications [16;17], wireless power transmission [18–20], and hybrid harvesters [21–23].

The first RF power transfer system has been developed by Brown et al. in NASA [24]. The researchers have been developed the first rectenna and achieved an efficiency of 40% by delivering 100 W to an electric rotor at a distance of more than 20 m and an operating frequency of 3 GHz. With the development of Schottky diodes capable of operating efficiently without an external bias at tens of GHz, low power RF energy harvesting systems have been designed during the 90s [25]. The RF energy harvesting

in ambient freely available RF sources has begun to evolve to meet the need for devices with low power requirements, and as shown in Figure 2.2, various antenna designs have been used.

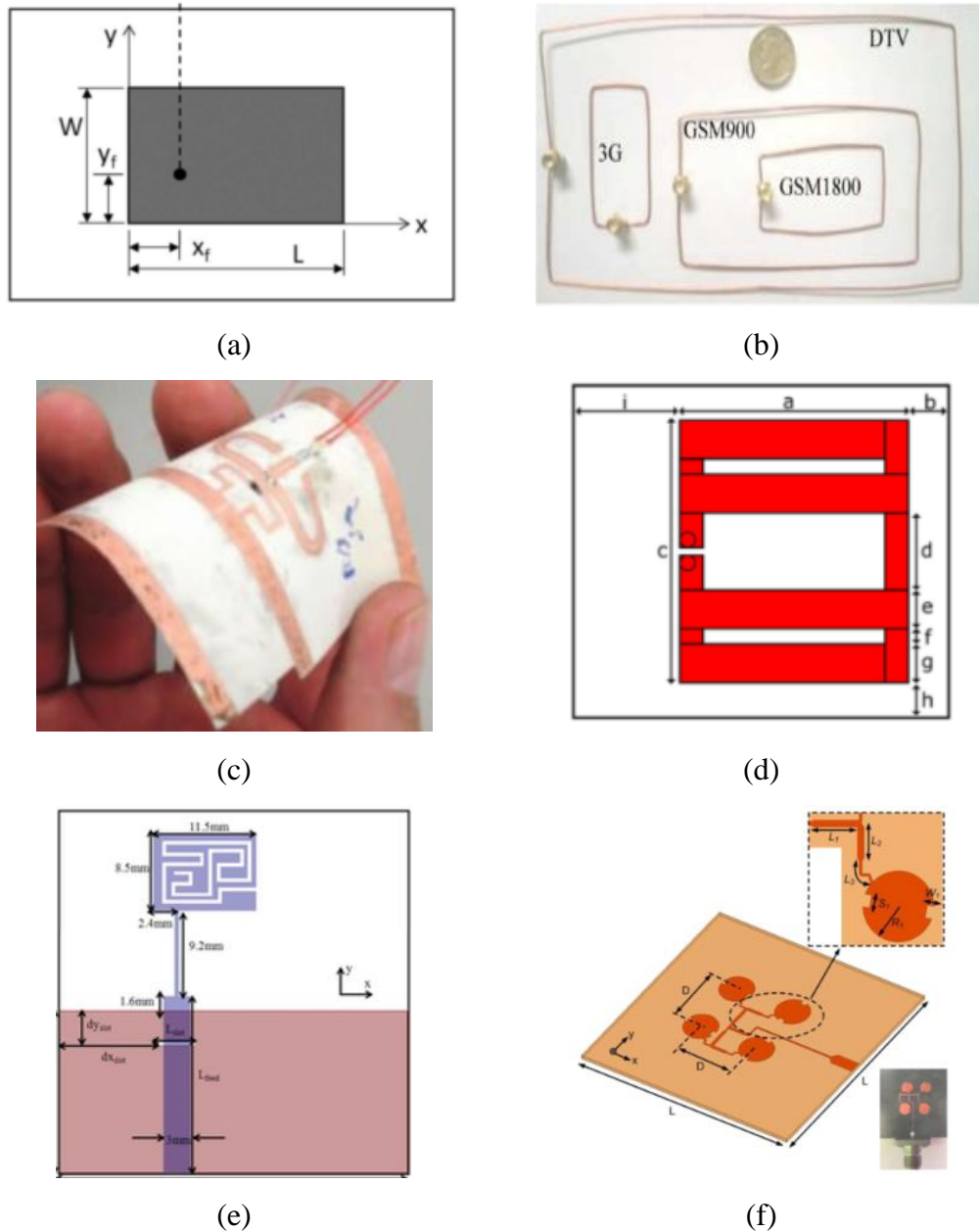


Figure 2.2 : Different antenna designs used for RF energy harvesting; (a) probe-fed microstrip patch antenna [26], (b) 50 Ω folded dipole antennas [27], (c) flexible yagi antenna [28], (d) small loop antenna [29], (e) anti-spiral slot resonator antenna [30], and (f) circular patch array antenna [31].

In [32], the study presented by Kim et al. have provided an overview of the ambient energy harvesting technologies (solar, thermal, radio frequency, and piezoelectric). In

this study, many studies on RF energy harvesting applications are investigated and proposed energy harvesting applications with different antenna (log-periodic, folded-dipole) and rectifying circuit designs. The researchers have been examined the RF performance of the surrounding area and determined operating bands, which is according to this data of the harvesting antenna. The fabricated system prototype which includes the antenna and rectifying circuit has appropriately operated.

In [33], the study has been presented an energy harvesting application which formed a one-sided flexible material by Kanaya et al., in 2013. This study includes energy harvesting antenna which operates at 900 MHz, the resonant circuit with tuning block, and rectifying circuit with 107Ω load. The RF-DC conversion efficiency has been obtained %58.7 as the simulation result and %44 as the measurement result which belongs to the fabricated prototype.

In [34], the study has been presented by Adami et al. wristband design for RF power harvesting. The proposed wristband design is flexible and has been comprised to operate at -24 dB input RF power in the 2.45 GHz operating band. The wristband design consists of a flexible RF energy harvesting antenna (which forms of the patch antenna) made of the woven polyester substrate and a rectifying circuit made of Rogers 5008 substrate. The efficiency of the wristband RF harvesting system has been obtained as %28.7 according to the input RF power value of -7 dBm.

In [35], self-sustained body area networks (BAN) sensor prototype which designed for human body self-monitoring and mobile healthcare has been presented by Yang et al. The prototype includes an electrically small triple band antenna which covers at GSM-900, UTMS-2100, and TD-LTE bands and rectifying circuit which designs for low power applications. Electrically small antenna gain values of 1 dBi, 2.64 dBi, and -0.19 dBi have been obtained at operating frequencies (0.9 GHz, 2.025 GHz, and 2.36 GHz), respectively. In the rectifying circuit, DC output power has been obtained at -10 dBm RF input power with %59 RF-DC conversion efficiency.

In [36], the study has been presented by Sun et al. an antenna array for RF power harvesting applications. The design of the proposed antenna array (1 x 4) consisting of a combination of 4 patch antennas have been designed to enhance beamwidth. With the aid of two auxiliary antennas, the beamwidth of the designed antenna array at the

H-plane is about two times wider as the typical antenna array (not enhanced beamwidth). The efficiency of the designed rectenna has been measured over 50% when the wave incident angle is between -38° and 35° .

In [37], broadband rectenna for ambient wireless energy harvesting applications has been presented by Song et al. The characteristics of the ambient radio-frequency energy have been investigated while the designing of a rectenna. A dual-polarized cross dipole antenna design has been proposed by researchers to be used as an energy harvesting antenna and to avoid frequency domain harmonics. A two-branch matching circuit is designed and fabricated to provide impedance matching between the energy harvesting antenna and RF to DC rectifying circuit.

In [38], the research work on a design, analysis, and optimization of RF energy harvesting system for GSM900 band (890–960 MHz) has been presented by Arrawatia et al. The differential microstrip antenna has a maximum gain of 8.5 dBi and VSWR ≤ 2 in the operating band. A rectenna which fabricated on a low-cost glass epoxy substrate is realized using a Schottky diode-rectifier and the developed differential antenna. In the rectenna's output load of 3 k Ω , DC output power was obtained at 2.19 dBm RF input power with %65.3 RF to DC conversion efficiency at 980 MHz.

In [8], the study presented by Kimionis et al. has provided 3-D inkjet printed (silver ink jetting) energy harvesting antenna design for RF harvesting sensor applications. The proposed antenna design is energized from two different ports and has carried about studies on isolation between these ports. Also, a rectifier circuit design has been put into the 3-D antenna structure, and a compact rectenna design has been created.

In [39], the study has been presented by Shen et al. a dual-port triple-band L-probe microstrip patch rectenna design for ambient RF energy harvesting operating at triple bands. The proposed rectenna system allows converting RF signals from different antenna ports and different operating bands (GSM-900, GSM-1800, and UMTS-2100 bands) to DC output power from all directions. As a result of the experiments when the power density is above 500 $\mu\text{W}/\text{m}^2$ in the environment, the efficiency of the dual-port triple-band rectenna system has been obtained over 40%.

In [40], the study on rectenna for energy harvesting application operating at ISM band has been presented by Chuma et al., in 2017. The proposed rectenna design consists

of a microstrip antenna based on fractal geometries and single stage voltage doubler rectifying circuit. The proposed antenna design has been fabricated using FR-4 substrate, and measurement results have been obtained similarly to the simulation results. In the rectifying circuit used Schottky SMS7630 diode, DC output power has been obtained at 2 dBm RF input power with ~62% RF-DC conversion efficiency.

In [41], the study has been presented by Song et al. a novel six-band dual circular polarization (CP) rectenna for RF power harvesting. Since the proposed antenna design operates in multiple bands, the rectenna design will also have a multi-band RF power input. Advanced impedance matching technique has been used to manage this RF power input efficiently in this study. The DC load resistance of the proposed energy harvesting system ranges from 10 to 75 k Ω , and the system DC power output values have been obtained 8 μ W and 26 μ W in indoor and outdoor environments, respectively.

In [42], the research study on a loop antenna with the artificial magnetic conductor for dual-band RF energy harvesting applications has been presented by Kamoda et al. The artificial magnetic conductor structure has been designed to produce a low profile high gain antenna and has been designed to operate in accordance with rectenna structure including loop antenna. In RF energy harvesting experiment, the output voltage of the proposed rectenna design has been obtained above 1.4 V when the load resistance is more extensive than about 70 k Ω for the continuous waves source and 90 k Ω for the actual modulated signal source.

In [43], the study has been presented by Marian et al. a wireless energy transfer system using microwave electromagnetic support. In this study, a novel rectenna design has been proposed which has the operating band can be tuned at 900 MHz and 2.45 GHz with high RF to DC conversion efficiency of %80. Also, the RF input power values of the rectenna system can range between -30 and 30 dBm.

In [44], the study on rectenna with the hybrid frequency selective surface for wireless power applications has been presented by Ferreira et al., in 2016. The proposed hybrid frequency selective surface design has been exhibited a bandpass frequency response at 900 MHz GSM band, band rejection frequency response at 2.4 GHz ISM band. The proposed rectenna design consists of an antenna array of 12 unit cells and a single

stage Greinacher rectifying circuit. In the rectenna output, average 300 μ W DC output power has been obtained at -10 dBm RF incident power level with 50% RF-DC conversion efficiency.

In [45], the research study on an ultra-wideband transparent antenna for photovoltaic solar-panel integration and RF energy harvesting applications has been presented by Peter et al. The energy harvesting antenna has been designed as a coplanar-waveguide (CPW) fed antenna sandwiched on a thin TCO polymer film with AgHT-4 substrate. The narrowband rectifying circuit has been developed using HSMS-2850 diode operating at a frequency of 2.55 GHz has been fabricated using FR-4 substrate. The harvesting performance of the rectenna design has been tested in an experiment made up of a horn antenna and a signal generator. Consequently, an average 18 mV DC output voltage has been obtained at -30 dBm input power.

In [46], the study has been presented by Popovic et al. on a system capable of harvesting energy from electromagnetic waves in the environment, where it is difficult to replace the batteries, and the energy sources are not known in location. The energy harvesting performance has been examined at 900 MHz and 2.45 GHz with the energy harvesting antenna as yagi-uda antenna array and rectifying circuit. RF-DC conversion efficiency and the highest output voltage on different loads (100 Ω to 63 k Ω) have been investigated, high resistance values for low RF power (-40 dBm) and low resistance values for high RF power (10 dBm) has been obtained as optimal values.

In the thesis conducted by Pinuela, RF energy harvesting, and inductive power transfer systems have been presented [47]. At the beginning of the study, the ambient RF source potential of London has been researched, and the thesis study which consists of designed various harvesters to cover four frequency bands from the most significant RF contributors within the UHF has been conducted according to the data obtained. The harvester prototypes have been tested on the London Underground stations and successful harvesting performance results have been obtained.

In the thesis conducted by Alloh, RF energy harvesting system designs, which are consists of the patch and array antennas and have been presented [48]. Proposed RF energy harvesting system has been designed to gather freely available GSM (GSM - 900 MHz) signals in the environment. In the proposed method, 7-stage voltage doubler

circuit using Schottky diodes has been used, and 2.283 V of DC output value has been obtained.

In the thesis conducted by Zhang, a study on rectenna designs analyzes, and measurements have been carried out [49] as an RF energy harvesting antenna has been used optimized broadband planar dipole antennas with a unidirectional radiation pattern in rectenna system. Also, it is presented that the desired DC output voltage with reasonable efficiency will have been obtained by composing rectenna array. The study has been presented that increasing the number of elements in the rectenna array, the higher output voltage, although the bandwidth is not as extensive as expected due to practical limits.

In the thesis conducted by Sim, RF energy harvesting system for low power embedded sensor networks which using at outdoor applications is presented [50]. The budget analysis of the proposed RF energy harvesting system has been carried out by finds out the advantages and disadvantages that may occur when applied to the sample sensor network (Zyrox2 Bait Station). Two different energy harvesting antennas (air-substrate-based folded shorted patch antenna and air-substrate-based folded shorted patch antenna with four slots) and a commercially available harvester module (P1110 Powerharvester) have been used in the study. RF energy harvesting system designs have been tested both in the laboratory and field.

In the thesis conducted by Brynhildsvoll, RF energy harvesting system operates at 900 MHz is presented [51]. The RF energy harvesting system with low power input consists of an antenna, a 3-stage rectifier circuit, and a boost converter circuit. The efficiency of the system which includes of antenna and rectifier circuit has been obtained 32.4 % (435 mV) and 19.6 % (184 mV) at input powers of -19 dBm and -23 dBm. After the boost converter circuit added, the efficiency of the system has been obtained 61.7 % (2.5 V) and 52.2 % (2 V) at rectifier output powers of -24 dBm and -30 dBm.

HSMS technology was used in the energy harvesting applications in [52] and [53], as an output 1.8 V (with 40 % RF-DC conversion efficiency at 900 MHz using HSMS-2850 diode), 0.77 V (with 83.73 % RF-DC conversion efficiency at 2.45 GHz using HSMS-2820 diode) DC voltage values have been obtained, respectively.

SMS technology was used in the energy harvesting applications in [54] and [55], as an output 0.4 V (with 40.8 % RF-DC conversion efficiency from 900 MHz using SMS-7630 diode) and 1 V (with 30 % RF-DC conversion efficiency at 2.45 GHz using SMS-7630 diode) DC voltage values have been obtained, respectively.

2.3 Ambient RF Energy Sources

The electromagnetic spectrum is the extent of all types of electromagnetic radiation. The radio frequency spectrum is the range between 3 Hz and 300 GHz of the electromagnetic spectrum, and the signals in this region are called the radio frequency signal. The signals that enable us to follow the TV and radio broadcasts reaching our homes are composed of the signals in this range. The scale of the electromagnetic spectrum that forms the RF spectrum and whose wavelengths varies between 1 mm and 100 km is presented in Figure 2.3.

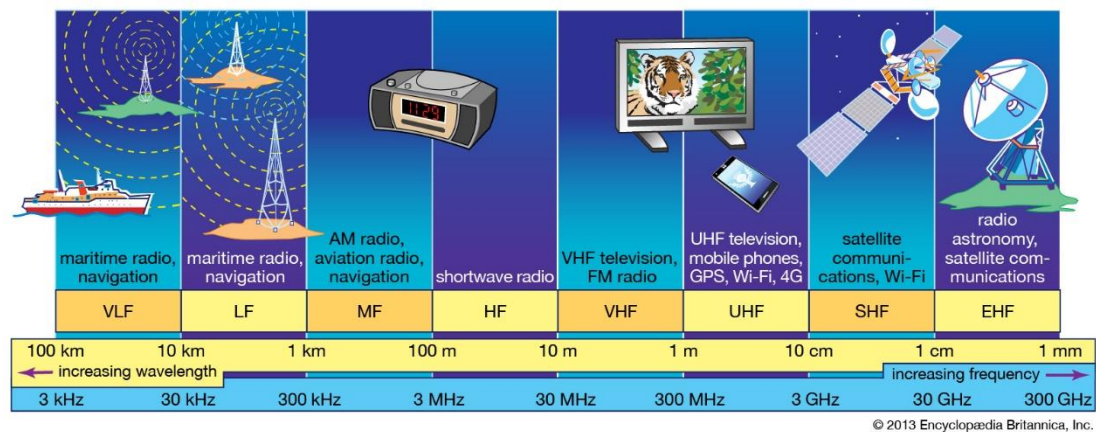


Figure 2.3 : Radio frequency spectrum [56].

Very high frequency (VHF) is the range of the electromagnetic spectrum between 30 MHz and 300 MHz. This frequency range is used for FM radio, TV and air traffic control broadcasts. Ultra high frequency is the range of the electromagnetic spectrum between 300 Mhz and 3 GHz. In this range, transmissions for global system for mobile communications 900 and 1800 (GSM-900 and GSM-1800), 3rd generation (UMTS-2100 or 3G), long term evaluation (LTE), industrial scientific medical (ISM) and Wi-Fi (wireless fidelity - 2.45 GHz) bands are located. The super high frequency (SHF) is the range of the electromagnetic spectrum from 3 to 30 GHz. This frequency range is

used for radar transmitters, microwave ovens, wireless LAN, mobile phones, satellite communications, and microwave radio relay connections.

RF energy harvesting systems use electromagnetic signals that radiate from various antennas as an RF signal source. RF signals are in sinusoidal forms, such as alternating current signals. RF radiation is generally quantified in terms of electric field strength, which is in V/m. In the far-field region, the electric field strength can be converted into incident power density using the following Equation 2.1 [57].

$$S = \frac{E^2}{Z_0} \quad (2.1)$$

where S is the incident power density (in W/m^2), E is electric field strength, and Z_0 is the impedance of free space (strN approximated by 377Ω). The radiated power in the far-field region can be calculated using the Friis' Transmission Equation (Equation 2.2) [57].

$$P_R = P_T G_T G_R \left(\frac{\lambda}{4\pi d} \right)^2 \quad (2.2)$$

where P_R is the radiated power (in watts), P_T is the transmitted power (in watts), G_T and G_R are the gain of the transmitting and receiving antenna, λ is the wavelength of the operating frequency (in meters), and d is the distance between the source and the energy harvesting antenna (in meters).

The power of the signal radiated from the RF source decreases until it reaches the RF energy harvesting system (path loss). Also, the path loss can be calculated using the Friis equation (Equation 2.3) [57].

$$L_p = 10 \log \left(\frac{4\pi d}{\lambda} \right)^2 \text{ (in dB)} \quad (2.3)$$

where λ is the wavelength of the operating frequency (in meters), d is the distance between the source and the energy harvesting antenna (in meters), and L_p is the free-space path loss in dB. The path loss in dB with increasing distance for 900 MHz and 2.4 GHz is shown in Figure 2.4.

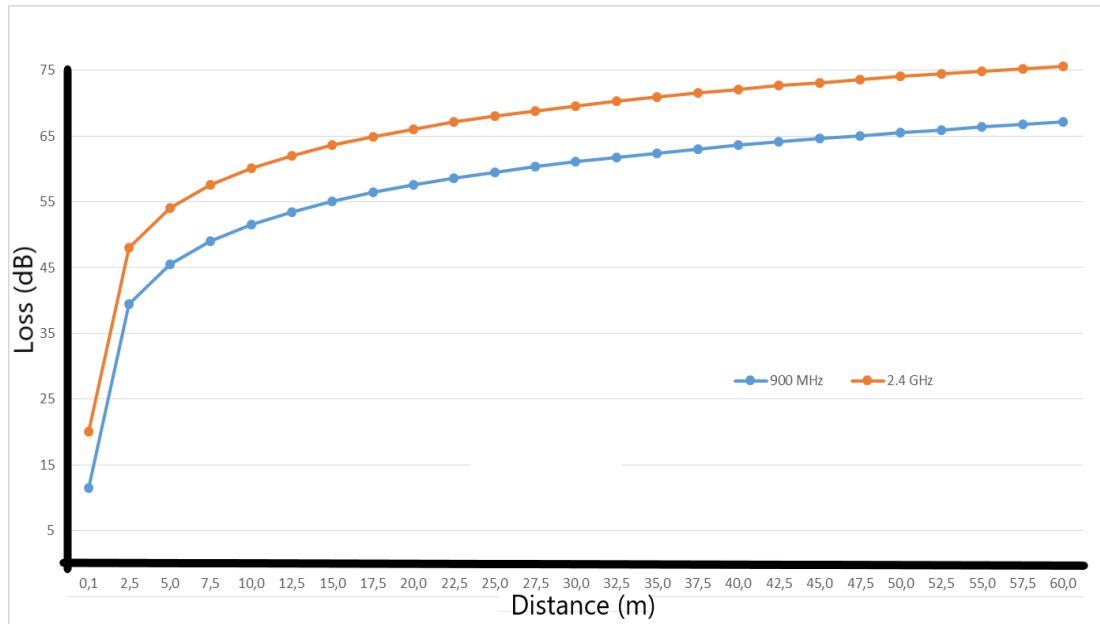


Figure 2.4 : The path loss in dB with increasing distance at 900 MHz and 2.4 GHz.

2.4 Antenna

An antenna (receiving antenna) is a vital component of an RF energy harvesting system, and it is responsible for gathering the RF signal from the radiating sources (transmitting antenna). The detailed literature review shows that different types of receiving antennas are used in RF energy harvesting systems. Receiving antennas are generally preferred in microstrip type due to their low profile physical properties and low fabrication costs [58]. Basic parameters determine the performance of a receiving antenna; input impedance, effective area, radiation pattern, gain, efficiency, and polarization type.

2.4.1 Antenna parameters

Antenna parameters are used to characterize the performance of an antenna when designing. Antenna regions, radiation pattern, gain, input impedance, bandwidth, and polarization that are the basic antenna parameters will be described in this section.

According to [57;59;60], the surrounding region of the antenna is divided into three regions as in Figure 2.5: the reactive near-field, the radiating near-field, and the far-field region. The boundaries separating these regions are unclear; these are depending on the length of the antennas and the wavelengths of the operating frequency. The first

region is Reactive Near-Field Region, which is the portion of the immediately surrounding the antenna [57]. The outer boundary of this region exists at a distance ($R < 0.62\sqrt{(D^3 / \lambda)}$) from the antenna surface, where λ is the wavelength, and D is the largest dimension of the antenna [57]. The second region is radiating Near-Field (Fresnel) Region that is the region of the field of an antenna between the reactive near-field and the far-field regions. In this region, radiation fields predominate. Also, this region does not occur if the antenna size is too large compared to the wavelength [57;59]. The boundary on the interval is taken to be the distance ($R \geq 0.62\sqrt{(D^3 / \lambda)}$) and the boundary on external the distance ($R < 2D^2 / \lambda$) [57]. The third region is the Far-Field (Fraunhofer) Region. Radiated electromagnetic waves from the antenna preponderate the far-field region. The far-field region exists at distances ($R > 2D^2 / \lambda$) from the antenna [57].

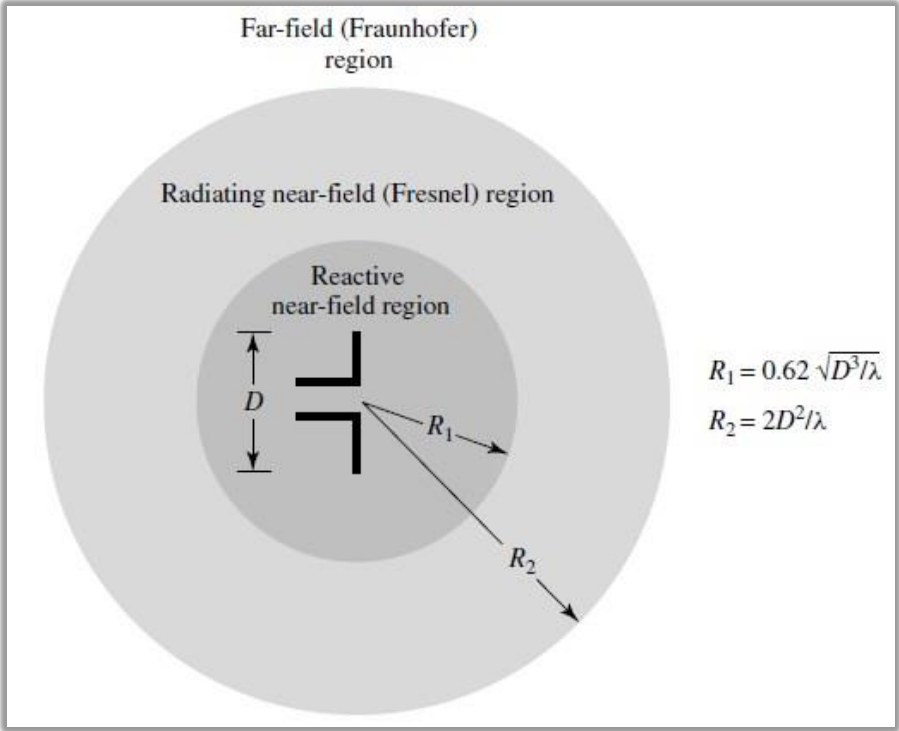


Figure 2.5 : Antenna field regions [57].

Directivity can be defined as the proportion of the radiation intensity in a given direction from the antenna to the radiation intensity averaged whole directions [57]. Also, directivity can be defined as a measure of the 'directional' of the radiation model

of an antenna. The directivity parameter can be explained by the given Equation 2.4 [57;59]:

$$D = D(\theta, \phi) = \frac{U(\theta, \phi)}{U_0} = 4\pi \frac{U(\theta, \phi)}{P_r} \quad (2.4)$$

where U is radiation intensity (W/solid angle), and P_r is the radiated power (in watts). The radiation intensity is defined as radiated power from an antenna per solid angle. The radiation intensity is a far-field parameter and can be explained by the given Equation 2.5 [57].

$$U = r^2 W_{rad} \quad (2.5)$$

where U is radiation intensity (W/solid angle), W_{rad} is radiation density (W/m^2), and r is distance (m).

Radiation power density is defined power density of an antenna in its far-field region. The tricenentary Poynting Vector S is identified as the power associated with an electromagnetic wave and can be explained by the given Equation 2.6 [57].

$$\vec{S} = \vec{E} \times \vec{H} \quad (2.6)$$

where \vec{E} is instantaneous electric field intensity (V/m) and H is instantaneous magnetic field intensity (A/m).

Total power crossing a closed surface can be obtained by integrating the standard component of the pointing vector over the entire surface, given in Equation 2.7 [57].

$$P = \iint_s S \cdot \vec{n} \, ds \quad (2.7)$$

where P is instantaneous total power crossing a closed surface (W), \vec{n} is unit vector normal to the surface, S is instantaneous Poynting vector (W/m^2), and ds is derivative of the area of the closed surface (m^2).

Antenna gain is the proportion of the radiation intensity in an expensed heading to the radiation intensity that would be achieved if the power postulated by the antenna were radiated isotropically and can be explained by the given Equation 2.8 [57;59].

$$Gain = 4\pi \frac{U(\theta, \phi)}{P_{in}} \quad (2.8)$$

where U is radiation intensity (W/solid angle) and P_{in} is the input (accepted) power (in watts). Also, antenna gain can be expressed as the ohmic losses in the antenna multiplied by directivity, given in Equation 2.9 [57;59].

$$Gain = G(\theta, \phi) = e_c e_d D(\theta, \phi) \quad (2.9)$$

where $D(\theta, \phi)$ is directivity of the antenna, e_c is conduction efficiency, and e_d is dielectric efficiency.

Antenna effective area of the receiving antenna is defined as the ratio of the available power at the terminals of an antenna to the power flux density of a plane wave incident on the antenna from that direction [57;60] and can be explained by the given Equation 2.10. Also, the effective area of the receiving antenna (A_{eff}) can be calculated by using the antenna gain and operating wavelength and can be explained by the given this equation [59].

$$A_{eff} = \frac{P_T}{W_\phi} = \frac{\lambda^2}{4\pi} Gain \quad (2.10)$$

where P_T is power delivered to the load (in watts), W_ϕ is power density of incident wave (W/m^2), and A_{eff} is effective area (m^2).

Antenna efficiency is used to consider losses at the input terminals and within the structure of the antenna and can be explained by the given Equation 2.11 [57].

$$e_0 = e_r e_c e_d \quad (2.11)$$

where e_0 is total efficiency (dimensionless), e_r is reflection (mismatch) efficiency, e_c is conduction efficiency, and e_d is dielectric efficiency. Also, reflection efficiency can be expressed in terms of reflection coefficient (Equation 2.12) [57].

$$e_r = 1 - |\Gamma|^2 \quad (2.12)$$

Reflection coefficient can be denoted in terms of antenna input impedance and transmission line impedance (Equation 2.13) [57;61]. Also, the voltage standing wave rate can be obtained by using the reflection coefficient (Equation 2.14) [57;59-61].

$$\Gamma = \frac{(Z_{in} - Z_0)}{(Z_{in} + Z_0)} \quad (2.13)$$

$$VSWR = \frac{1 + |\Gamma|}{1 - |\Gamma|} \quad (2.14)$$

where Γ is the voltage reflection coefficient at the input terminal of the antenna, Z_{in} is antenna input impedance, and Z_0 is the impedance of the transmission line.

Also, the antenna efficiency can be calculated by Equation 2.15 using the reflection coefficient [57].

$$e_0 = e_r e_c e_d = e_r e_{cd} = e_{cd} (1 - |\Gamma|^2) \quad (2.15)$$

Antenna bandwidth is identified as the sequence of frequencies within which the performance of the antenna, concerning some characteristic, conforms to a specified standard [57]. The antenna bandwidth is usually expressed as the ratio of the upper-to-lower frequencies of acceptable operation [57].

Polarization is identified as the orientation of the electric field of an electromagnetic wave [57;59]. Polarization types occur depending on the magnitude and destination components of the electric field of electromagnetic waves. There are two kinds of polarization, linear and elliptical. It also has circular polarization as a special type of elliptic polarization. Polarization types are presented in Figure 2.6.

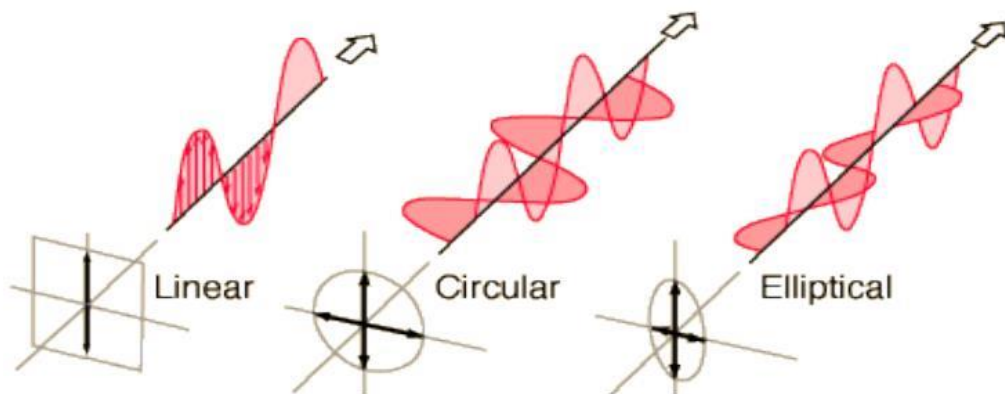


Figure 2.6 : Antenna polarization types [60].

Antenna input impedance is defined as the impedance an antenna at its terminals, which the proportion of the voltage to current at a couple of antenna input terminals [57]. Antenna equivalent model is shown in Figure 2.7.

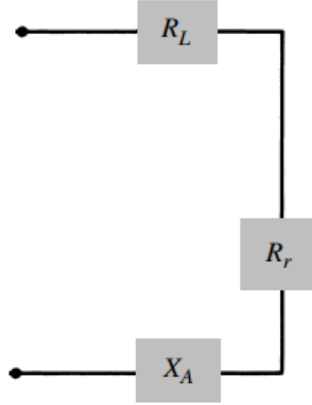


Figure 2.7 : Antenna equivalent model.

Antenna input impedance (Z_A) can be calculated by Equation 2.16 using the radiation resistance (R_r), loss resistance (R_L), and antenna reactance (X_A) [57].

$$Z_A = R_A + jX_A = R_r + R_L + jX_A \quad (2.16)$$

2.5 Impedance Matching Circuit

In an RF energy harvesting system, an energy harvesting antenna gathers the incident RF signals, an impedance matching circuit steps up the power transfer from the antenna to the rectifying circuit, and rectifying circuit rectifies the gathering RF signals to output DC voltages. The input impedance of the receiving antenna is 50Ω because it is generally determined compatible with the line impedance. The input impedance of the RF-DC rectifier circuit has a reactive value due to the diodes and capacitors used in the voltage multiplier circuit. For this reason, the impedance mismatch between the receiving antenna and the RF-DC rectifying circuit is prevalent. Impedance matching circuit is vital in optimizing the performance of the RF energy harvesting system [62].

There is a need for an impedance matching network to obtain maximum power transfer between the RF energy harvesting system components (RF energy harvesting antenna

and rectifying circuit) with different impedance values. A matching network between the antenna (V_A , Z_A) and the rectifying circuit (Z_R , V_R) shown in Figure 2.8.



Figure 2.8 : Matching network between the antenna and the rectifying circuit.

where V_A is the antenna voltage, and Z_A is the antenna impedance (Equation 2.15). V_R is the voltage, and Z_R is the input impedance of the rectifying circuit. Z_{in} is the impedance seen looking into the matching network.

In the case of a lossless matching network, all output RF power from the antenna is transmitted to the rectifying circuit. The maximum power transfer occurs when the impedance value seen looking at the matching network (Z_{in}) is come up to the complex conjugate of the antenna impedance (Z_A^*). Maximum power transfer condition is shown in Equation 2.17.

$$Z_{in} = Z_A^* \rightarrow Z_{in} = R_A - jX_A \quad (2.17)$$

There are several possible difficulties in designing an impedance matching network for RF energy harvesting system. The frequencies and magnitudes of RF signals from the antenna are continually changing according to various physical factors, so an impedance matching solution must be produced in broadband. Also, the RF energy harvesting system is a non-linear system because of the input of rectifying circuit (input impedance and input power), and the output of antenna (output power and output impedance) changes as a function of operating frequency. To achieve maximum power transfer between the antenna and the rectifying circuit, an impedance matching network should be designed by adjusting the antenna output power to a minimum to ensure correct and proper operation of the RF energy harvesting system. The antenna output impedance will continuously vary due to the antenna's physical conditions, so the constant or specific capacitance or (and) inductance values of the impedance matching circuit will not be a continuous solution. To overcome changing antenna input impedance, the tunable impedance matching solution has been used [14;63].

2.6 Rectifying Circuit

The rectifying circuit plays a vital role in RF energy harvesting systems and has rewarded many awards and achievements that demonstrate the importance of relevant studies in our modern life [64]. An RF-DC rectifying circuit converts the captured RF signals (AC type) from the receiving antenna and provides a DC output voltage to the DC load. A significant challenge of the rectifying circuit design is to generate DC voltage from little input RF power [3].

Rectifier technologies are examined in two main categories as diode based and transistor based rectifier circuits. However, transistor-based rectifier circuits are developed based on diode effects [65]. The diode is the main component of a rectifying circuit. The efficiency of the rectifying circuit is essential and defined in Equation 2.18,

$$\eta = \frac{P_{DC}}{P_{RF}} \quad (2.18)$$

where P_{DC} is the DC power out of the rectifying circuit and P_{RF} is the power available at the input of the rectifying circuit.

A half-wave rectifier circuit in Figure 2.9 can be designed simply by using a diode. The input of the rectifier circuit is in the form of an AC signal consisting of the negative and positive cycle. On the positive half cycle of the AC signal, the diode is forward biased and current flowing through the diode, charging the capacitor. On the negative half cycle of the AC signal, the diode is reverse biased, and no current flows through the diode or circuit.

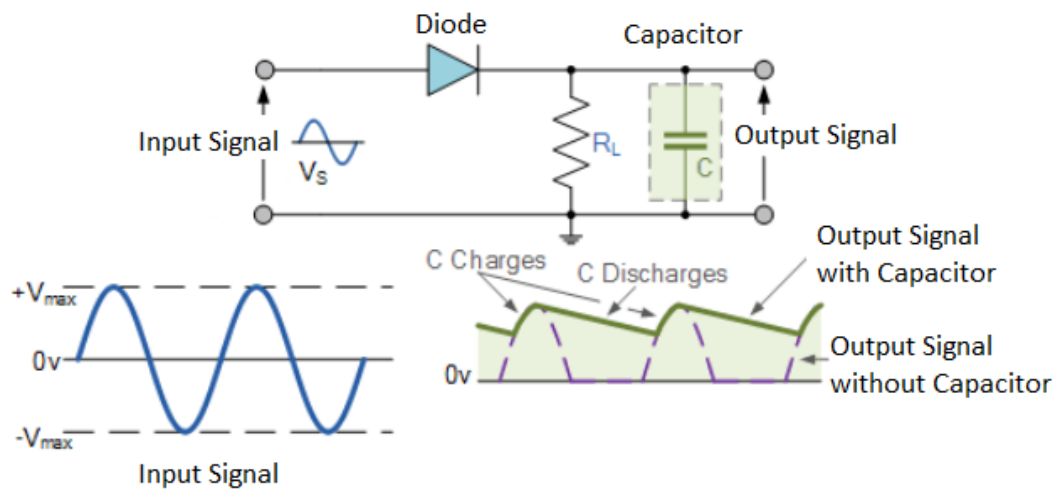


Figure 2.9 : Half-wave rectifier.

A full-wave rectifier in Figure 2.10 can be designed simply by using two diodes. On the positive half cycle of the AC signal, when the D_1 diode is forward biased, D_2 is reverse biased, and the current is flowing to R_L . On the negative half cycle of the AC signal, when the D_1 diode is reverse biased, D_2 is forward biased, and the current is flowing to R_L . A purer DC output signal is obtained in the full-wave rectifier circuit than the half-wave rectifier circuit. Also, using the capacitor in the full-wave rectifier circuit (due to the effect of the capacitor discharge) a purer DC output signal can be obtained (Figure 2.10).

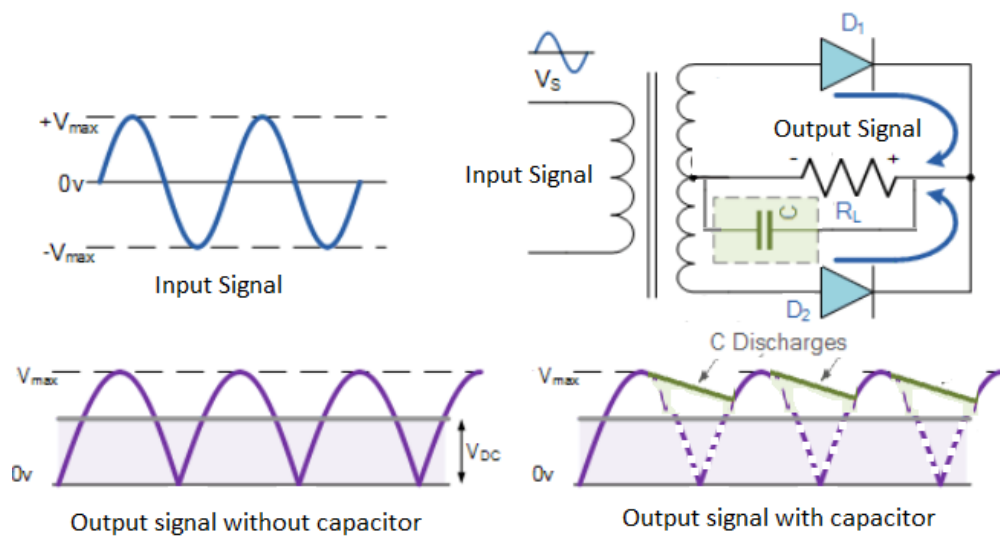


Figure 2.10 : Full-wave rectifier.

The most critical circuit element of the rectifier circuit is the diode, so the selection of the correct diode type is very significant. Schottky diodes have fast switching times (low reverse-recovery time), the low forward voltage drop (typically 0.25 to 0.4 volts for a metal-silicon junction), and low junction capacitance [66]. Schottky diodes are made of a metal-to-N terminal instead traditional diodes are constructed of a P-N semiconductor junction. The equivalent electrical circuit of a Schottky diode is shown in Figure 2.11 (C_j is junction capacitance in Farad, R_s is the bulk resistance in Ohm, and R_j is the junction resistance in Ohm).



Figure 2.11 : Equivalent circuit of a Schottky diode [67].

The Schottky diodes have two main classes. The first class is the n-type silicon with a high barrier and low values of series resistance (R_s). The second one is the p-type silicon characterized by a low barrier and high values of series resistance (R_s). P-type Schottky diodes are used because of their low series resistance for RF energy harvesting applications (100 times lower compared to n-type) [68]. To obtain the maximum DC output, the entire incoming RF signal should ideally appear across R_j with no losses over R_s [48].

The operation of a voltage doubler can be explained by looking at successive half cycles of an RF input signal. The input RF signal (in AC form) is rectified in the positive semi of the input cycle, followed by the negative semi of the input cycle. However, the voltage stored on the input capacitor during the one-half cycle is transmitted to the output capacitor during the next half cycle of the input signal. Thus, the voltage on the capacitor at the output is approximately two times the peak voltage of the RF source minus the diode turn-on voltage. A single stage Villard voltage

doubler circuit, in which each stage consists of two capacitors and two diodes (Figure 2.12).

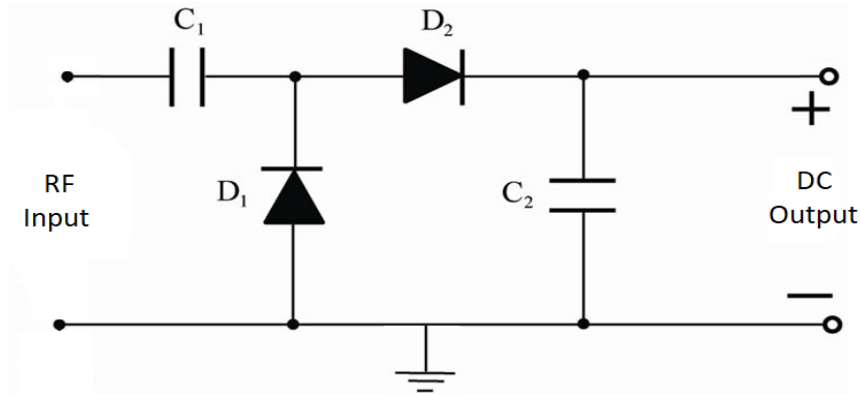
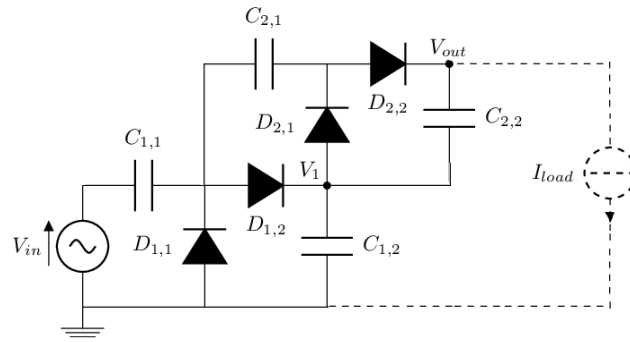


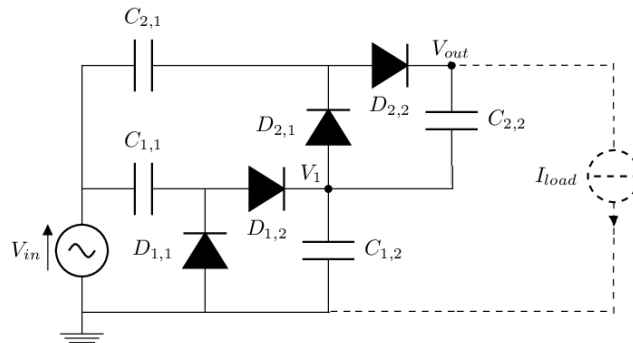
Figure 2.12 : Single stage Villard voltage doubler circuit.

Voltage multiplier topologies have been proposed and tested for RF energy harvesting applications in literature such as Greinacher rectifier invented by Heinrich Greinacher in 1919, Villard voltage rectifier also referred as Cockroft-Walton voltage rectifier designed by John Cockroft and Ernest Walton, and Dickson rectifier designed by Donald Dickson. This circuit performs not only the RF to DC conversion, but also produces a DC output voltage that multiplies the peak amplitude of the incoming RF signal.

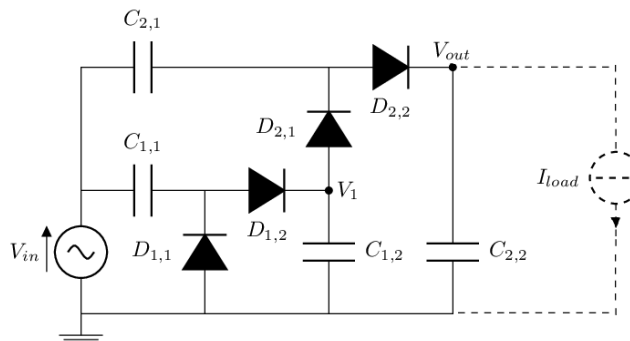
Villard voltage multiplier topology is commonly employed in rectifying circuits that expect low input RF signals during operation [69]. The Greinacher voltage multiplier topology is essentially a Villard multiplier topology, with the addition of a peak-detector rectification stage at the output. The Dickson multiplier topology, another topology often mentioned in the RF energy harvesting applications, is an adaptation of the Greinacher and Villard topologies, with the distinction of requiring a DC input signal for operation [69]. The 2-stage Villard voltage rectifier (Figure 2.13.a), 2-stage Greinacher voltage rectifier (Figure 2.13.b), and 2-stage Dickson voltage rectifier circuits are shown in Figure 2.13.



(a)



(b)



(c)

Figure 2.13 : Different voltage rectifier topologies:

- (a) 2-stage Villard voltage rectifier, (b) 2-stage Greinacher voltage rectifier, and
 (c) 2-stage Dickson voltage rectifier.

In the voltage multiplier circuits, diodes are selected close to the ideal (no threshold voltage or loss) and the capacitor values as high as possible. The capacitor values selected as high values ensure that the voltage in the capacitor charge does not change significantly when the capacitor is charged or discharged.

An attractive feature of these rectifier circuits is that it can be arranged in a cascade configuration to achieve higher output DC voltage. An N-Stage voltage multiplier circuit shown in Figure 2.14.

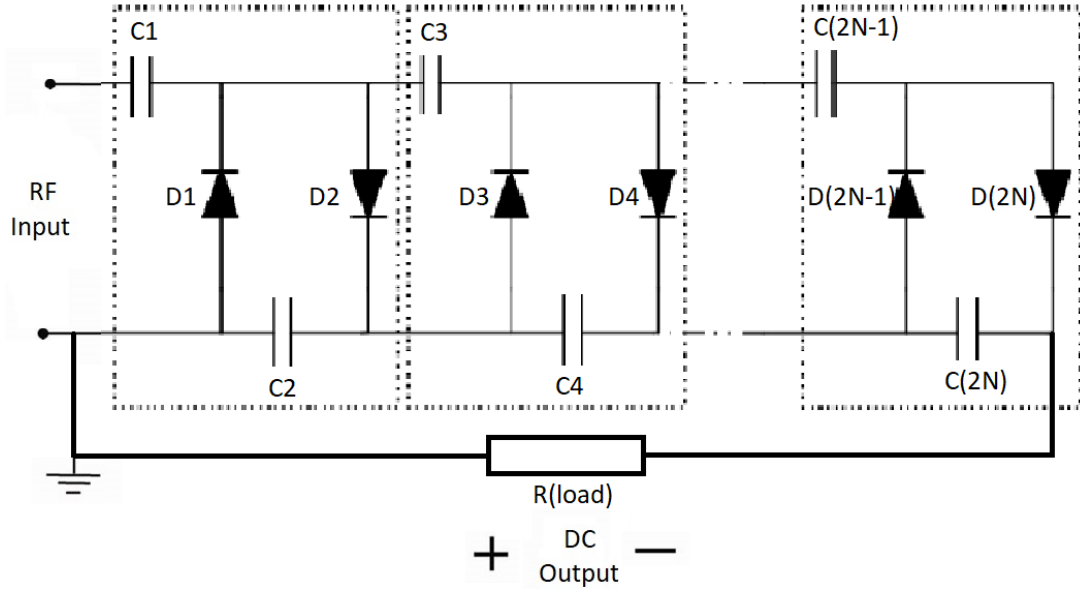


Figure 2.14 : N-Stage voltage rectifier.

The higher output DC voltage can be obtained by increasing the number of voltage multiplier circuit stages. Even if the low RF signal is used as input, a suitable multistage voltage multiplier circuit can be designed to obtain the desired DC output voltage. As the stage number increases, the DC output voltage increases until it reaches an optimal point. Adding more stages beyond the optimal point reduces the quality factor (due to the linearly increased parasitic capacitance), and it causes a decrease in DC output voltage [62]. Therefore, it is vital that the number of rectifier stages is determined through circuit simulation, and to be designed simultaneously with the impedance matching network, to maximize the DC output voltage, maintain a high system quality factor and optimize the power conversion efficiency.

2.7 DC Load

One of the crucial parts of RF energy harvesting applications is the output DC load part. The DC load part at the end of the energy harvesting circuit generally consists of devices or devices with low power consumption. The low power device in the DC load part has its internal resistance (R_{LOAD}), and this resistance value affects the equivalent

impedance values of the RF-DC rectifying circuit and the matching circuit. The DC load resistance in the RF energy harvesting system is presented in Figure 2.15.

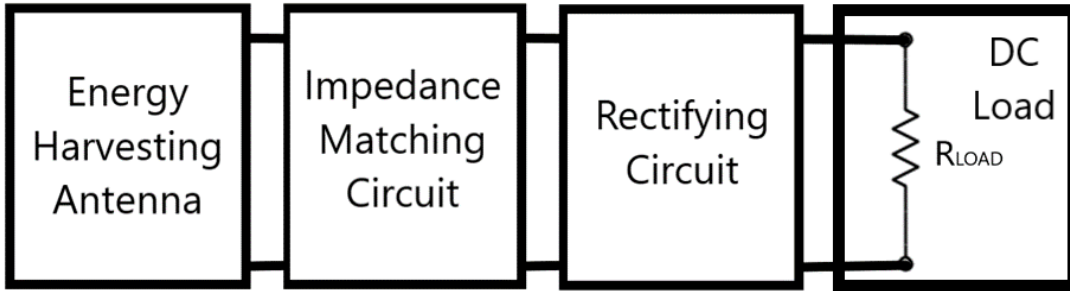


Figure 2.15 : RF energy harvesting system with DC load resistance.

The design of the RF energy harvesting application designed to compensate for the power requirement of the device requiring low power consumption must be determined in advance.

As the RF energy harvesting system is nonlinear, the output DC voltage value will change to nonlinear depending on the resistance value of the DC load part. Therefore, the load resistance of the DC load part must be considered at the beginning of the RF energy harvesting system designing.

2.8 RF Energy Harvesting System Efficiency

The RF to DC conversion efficiency of the RF energy harvesting system is defined as the ratio of the output power P_{out} over the input power P_{in} , means the conversion efficiency of the system is the DC power at the DC Load over the RF input gathered by the energy harvesting antenna (Equation 2.19).

$$\eta = \frac{P_{out}}{P_{in}} = \frac{(V_{DC})^2}{R_{load} A_{eff} P_d} \quad (2.19)$$

where P_d is the maximum power density at the center of an antenna aperture (W), V_{DC} is the output power of the RF energy harvesting system.

3. RF ENERGY HARVESTING SYSTEM DESIGN CONSIDERATIONS

In this section, two different rectenna designs which could be used in RF energy harvesting systems have been presented. The designed energy harvesting antennas is a microstrip structure. Energy harvesting antenna, impedance matching, and RF to DC rectifying circuit designs operate in different operating bands (900 MHz and 2.4 GHz). There are different impedance matching circuits and different rectifying circuit design for each energy harvesting antenna designs. The components of the energy harvesting system operate in the same band. Also, because the DC load impedance values are different in the same frequency-operated energy harvesting antenna designs, various performance parameters are composed for the impedance matching and RF to DC rectifying circuit designs.

Several studies on RF energy harvesting in the literature have been investigated. The acquired data as a result of the literature review are presented in Table 3.1 (for 900 MHz) and Table 3.2 (for 2.4 GHz).

Table 3.1 : Literature review of RF energy harvesting systems operating at 900 MHz.

Reference Number	Physical Dimensions [mm]	Gain	Center Frequency (Bandwidth)	Operating Frequency Band	RF to DC Conversion Efficiency	Output Voltage
[70]	128 x 110 x 0.8	2.29 dBi	848 MHz (21 MHz)	839-860 MHz	not specified	not specified
[71]	240 x 240 x 264	9.1 dBi	900 MHz (121 MHz)	877-998 MHz	not specified	not specified
[72]	120 x 55 x 0.5	2.05 dBi	915 MHz (300 MHz)	850-1150 MHz	not specified	not specified
[73]	172 x 38 x 13	3 dBi	878 MHz (47 MHz)	839-860 MHz	not specified	-11 dBm: 1.08 V
[74]	120 x 50 x 1.6	1.97 dBi	915 MHz (124 MHz)	853-977 MHz	not specified	-20 dBm: 30 mV
[62]	not specified	6 dBi	915 MHz (26 MHz)	902-928 MHz	-22 dBm: 60 %	not specified
[75]	77 x 36 x 1.6	2.12 dBi	900 MHz	not specified	-20 dBm: 23.8 %	not specified
[76]	100 x 128 x 1.6	1.81 dBi	900 MHz	not specified	not specified	not specified
[77]	130 x 140 x 0.25	3.6 dBi	900 MHz (200 MHz)	780-980 MHz	-10 dBm: 65 %	not specified
[78]	106 x 100 x 1.6	1.82 dBi	1 GHz (230 MHz)	0.9-1.13 GHz	-20 dBm: 18.2%	not specified

Table 3.2 : Literature review of RF energy harvesting systems operating at 2.4 GHz.

Reference Number	Physical Dimensions [mm]	Gain	Center Frequency (Bandwidth)	Operating Frequency Band	RF to DC Conversion Efficiency	Output Voltage
[79]	35 x 35 x 3.7	4.6 dBi	2.4 GHz (140 MHz)	2.35-2.49 GHz	-10 dBm: 28%	not specified
[80]	64 x 70 x 3.63	7.6 dBi	2.45 GHz (20 MHz)	2.44-2.46 GHz	-20 dBm: 33.6%	not specified
[75]	77 x 36 x 1.6	not specified	2.4 GHz (64 MHz)	2.37-2.43 GHz	-20 dBm: 23.8%	not specified
[81]	64 x 100 x 1.57	5.7 dBi	2.4 GHz	not specified	not specified	-20dBm: 412 mV
[81]	45 x 45 x 0.8	1.5 dBi	2.45 GHz (1.3 GHz)	1.95-3.25 GHz	12 dBm: 73.7 %	not specified
[53]	38 x 29.5 x 1.6	5 dBi	not specified	not specified	-21 dBm: 83.7 %	not specified
[82]	85 x 100 x 8.2	7.68 dBi	not specified	not specified	20 dBm: 78.7 %	not specified
[83]	160 x 160 x 30	7.96 dBi	2.4 GHz (1.9 GHz)	1.7-3.6 GHz	not specified	not specified
[84]	19 x 14.5 x 0.76	11.4 dBi	2.4 GHz (340 MHz)	2.26-2.6 GHz	-25.4 dBm: 86 %	not specified
[41]	110 x 90 x 1.6	6.31 dBi	2.45 GHz (1.95 GHz)	0.55-2.5 GHz	-5 dBm: 67 %	not specified

3.1 RF Survey

Based on the goal of the survey or system analysis, different measuring devices can be used to measure the transmitted RF signals in freely available in the environment. There are mainly three different devices to measure these signals; survey meters, personal dosimeters, and spectrum analyzers [47]. Survey meters (in Figure 3.1.a) are used to measure RF signals in near-field and far-field, can demonstrate results in broadband but do not give any information about the signal and modulation type. Personnel dosimeters (in Figure 3.1.b) are designed to operate at specific frequencies and by particular standards, indicating the result obtained at certain frequencies to the user as a percentage by the limits of the established criteria. Spectrum analyzers (in Figure 3.1.c) are used to measure RF signals in near-field and far-field, showing precise and stable results in a narrow band. It gives the frequency and power information at a single point or desired range according to the operating limits of the device.



Figure 3.1 : RF signal measurement devices: (a) Survey meter, (b) Personnel dosimeter, and (c) Spectrum analyzer.

In the design procedure of an RF energy harvesting system, the system's operational area, the antenna's operating band or the bands, the amount of RF power in the system's operational area and the required power need for devices must be decided. The functional characteristics of the RF energy harvesting system will be determined and limited according to these data.

The operating frequencies of the RF energy harvesting systems designed in this study have been chosen based on the RF signal sources, which are quite common in the

environment. One of these systems has been designed to operate in the GSM band (900 MHz) while the other system designed to operate in the ISM band (2.4 GHz).

3.2 Rectenna Design – 1

The proposed Rectenna Design – 1 consists of an energy harvesting antenna, impedance matching circuit, and rectifying circuit. The energy harvesting system is designed to energizing the KY – 028 digital temperature sensor [85] (DC Load).

3.2.1 Energy harvesting antenna design

The energy harvesting antenna design consists of the split-ring resonator structure on the top and the framed elliptic structure on the ground surface. The port connection is from the end of the ring resonator in the top side to the elliptical structure in the bottom surface, which is directly fed through the probe feeding technique. The proposed energy harvesting antenna modeled in CST Studio Suite [86] using Rogers RO4003C [87] substrate with a thickness of 1.52 mm with 0.035 mm copper in both surfaces. The substrate material has a dielectric constant of 3.38 and a loss tangent of 0.0027. Also, the energy harvesting antenna design modeled in CST Studio Suite has been prototyped with PCB printing circuit device using Rogers 4003C substrate material. The top and bottom surfaces of the energy harvesting antenna design are shown in Figure 3.2 with the design parameters. In the same figure, the prototype fabricated using Rogers RO4003C substrate is also presented.

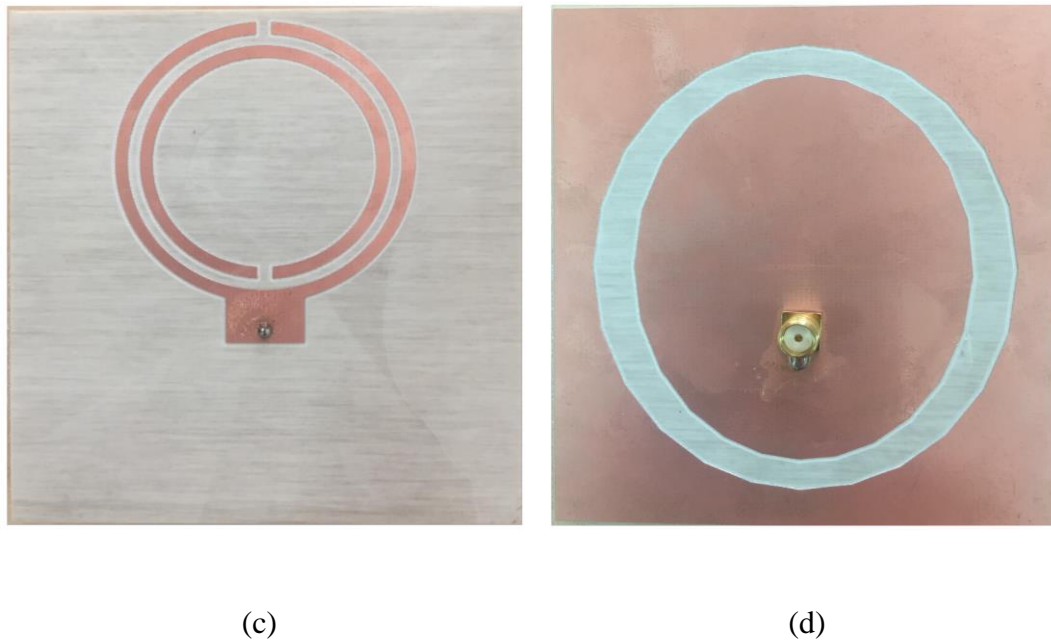
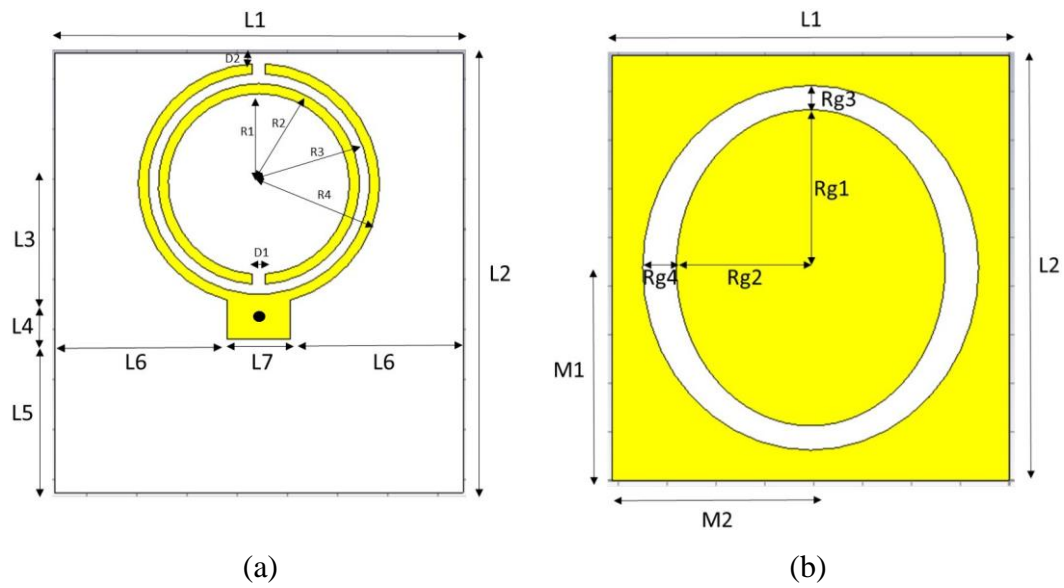


Figure 3.2 : (a) top and (b) bottom surfaces of energy harvesting antenna model with design parameters (The relevant dimensions are (in mm); $R1=18$, $R2=20$, $R3=22$, $R4=24$, $D1=2.5$, $D2=2$, $L1=81.25$, $L2=87.5$, $L3=23$, $L4=8.2$, $L5=30.1$, $L6=34.375$, $L7=12.5$, $M1=43.75$, $M2=40.625$, $Rg1=32.5$, $Rg2=27.5$, $Rg3=5$, $Rg4=6.5$, \bullet is feeding point), (c) top, and (d) bottom views of the fabricated prototype of energy harvesting antenna design.

3.2.2 Impedance matching and RF to DC rectifying circuit design

The RF to DC rectifying circuit of the RF energy harvesting system is a one stage Villard voltage rectifier topology. The RF energy harvesting system model is shown in Figure 3.3.a.

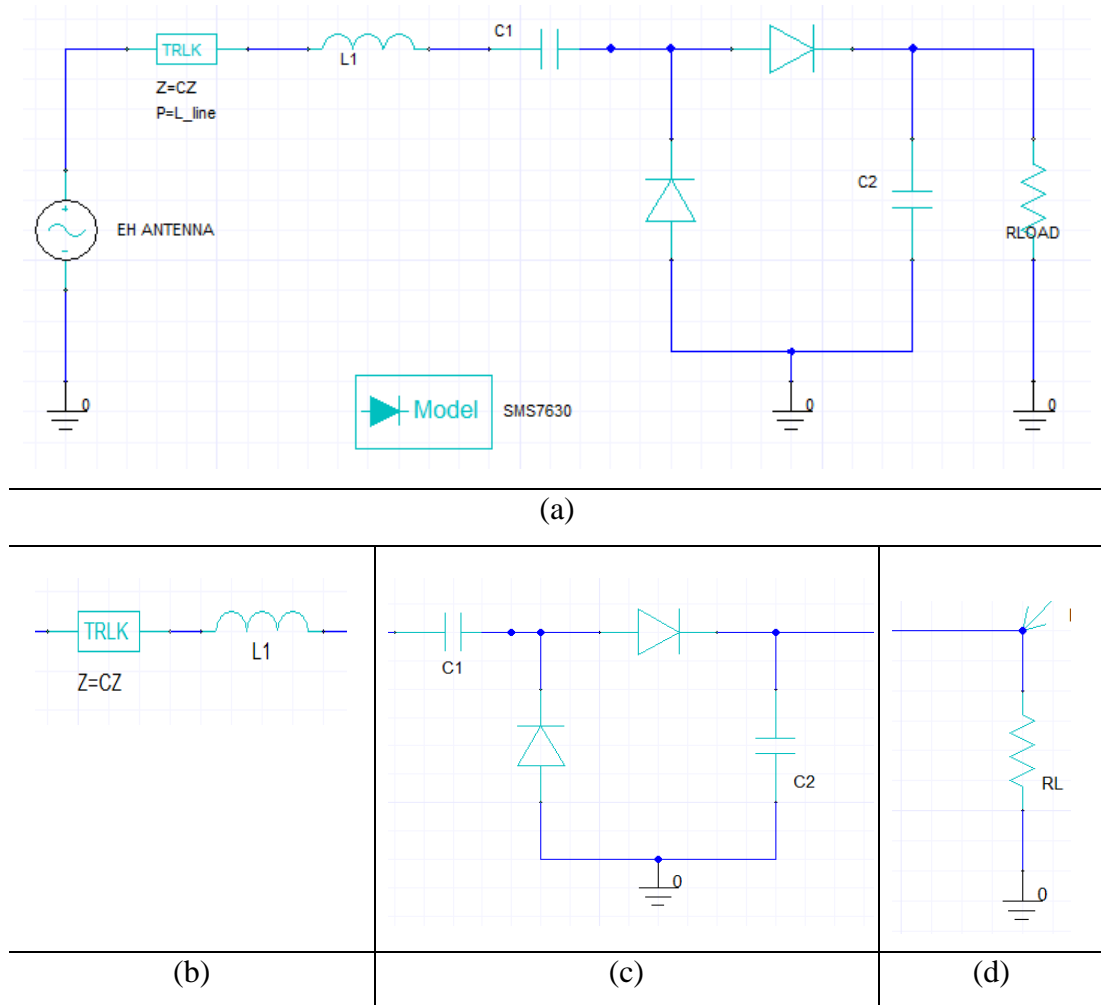


Figure 3.3 : (a) Configuration of the proposed RF energy harvesting system (antenna, matching circuit, rectifying circuit, and DC load), (b) matching circuit (c) Villard voltage rectifier circuit, and (d) DC load (temperature sensor).

The impedance matching circuit is designed to match the antenna and RF to DC rectifying circuit input impedance. The impedance matching circuit consists of an inductive element and a $\lambda / 4$ impedance transformer. The impedance matching circuit is shown in Figure 3.3.b. Rectifying circuit has been designed for obtaining DC output voltage from the gathered RF signal operates at 900 MHz resonance frequency, which

consisting of two diodes and two capacitors in a single stage Villard voltage rectifier topology have been composed. The Villard voltage rectifier circuit is shown in Figure 3.3.c. A rectifying circuit based on zero bias Schottky detector diode SMS 7630 Skyworks [88], and impedance matching circuit has been designed with the numerical model in Ansoft Designer and Ansys Electronics Desktop [89]. The end of the impedance matching and RF to DC rectifying circuit is load resistance. The value of the DC load is the resistance value of the temperature sensor and the design parameters of the impedance matching and RF to DC rectifying circuit is based on this DC load resistance value. The DC load is shown in Figure 3.3.d.

In the RF to DC rectifying circuit, zero biased Schottky barrier diode SMS 7630 have been used. The Spice parameters of the SMS 7630 used the nonlinear simulation are presented in Table 3.3.

Table 3.3 : Skyworks SMS 7630 Spice parameters.

Is (A)	Rs (Ω)	N	TT (sec)	Cjo(pF)	M
5×10^{-6}	20	1.05	10^{-11}	0.14	0.4
XTI	Fc	Bv (V)	IBV (A)	Vj (V)	EG (eV)
2	0.5	2	10^{-4}	0.34	0.69

The DC load resistance is quite similar to the input resistance of the commercial temperature sensor, KY-028 Digital Temperature Sensor. The lumped circuit element values of the impedance matching and RF to DC rectifying circuit with DC Load are listed in Table 3.4.

Table 3.4 : Design parameters of proposed impedance matching and RF to DC rectifying circuit with DC load.

Z line (CZ)	L line	L1	C1	C2	R load
77.45 Ω	44.5 mm	150nH	1.5nF	5.6nF	50 K Ω

3.3 Rectenna Design – 2

The proposed Rectenna Design – 2 consists of an energy harvesting antenna, impedance matching circuit, and rectifying circuit. The RF energy harvesting system has been designed to be efficient in different resistance values for use in different loads.

3.3.1 Energy harvesting antenna design

The proposed energy harvesting antenna modeled using Rogers RO4003 substrate in CST Microwave Studio. The substrate material 1.52 mm thick with the dielectric constant of 3.38 and loss tangent of 0.0027. The top layer of the energy harvesting antenna consists of a U-shaped structure directly connected to the feeding line and a T-shaped structure which is designed with a hole in the middle and no connection to the U-shaped structure. The bottom layer of the energy harvesting antenna consists of two same structures which are located at the upper and lower, and thin connection paths connecting these two structures from the antenna boundaries. The top and bottom of the energy harvesting antenna model are shown in Figure 3.4 with the design parameters. In the same figure, the prototype fabricated using Rogers RO4003C substrate is also presented.

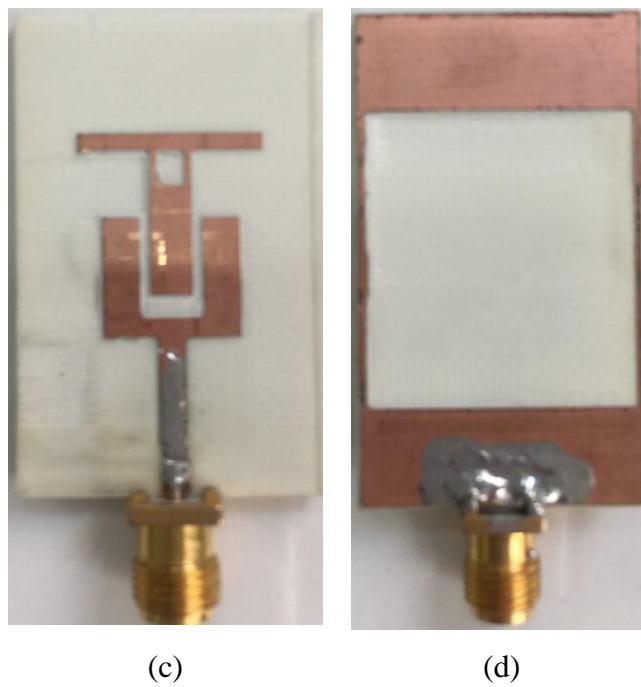
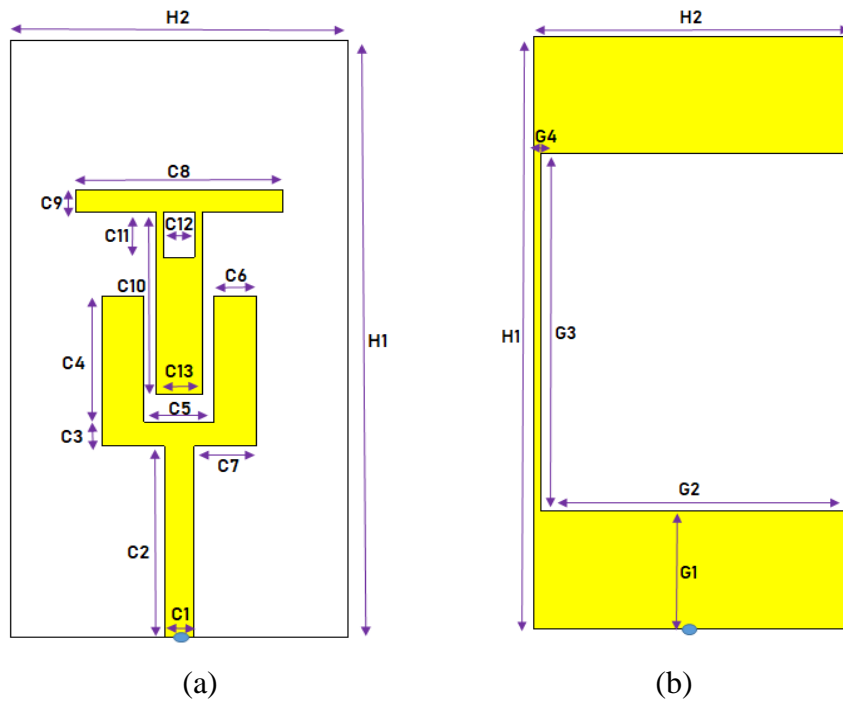


Figure 3.4 : (a) top and (b) bottom layers of energy harvesting antenna model with design parameters (The relevant dimensions are (in mm); $H1=41.8$, $H2=22$, $C1=1.9$, $C2=13.4$, $C3=1.7$, $C4=8.8$, $C5=4.6$, $C6=2.7$, $C7=4$, $C8=13.5$, $C9=1.5$, $C10=12.8$, $C11=3.2$, $C12=2$, $G1=8.3$, $G2=21$, $G3=25.2$, $G4=0.5$, and \bullet are feeding points), (c) top, and (d) bottom views of the fabricated prototype of energy harvesting antenna design.

3.3.2 Impedance matching and RF to DC rectifying circuit design

The RF to DC rectifying circuit of the RF energy harvesting system is a one stage Villard voltage rectifier topology. An RF to DC rectifying circuit based on zero bias Schottky detector diode SMS 7630 Skyworks and impedance matching element (circuit) has been designed with the numerical model in Ansys Electronics Desktop. The RF energy harvesting system model is shown in Figure 3.5.a.

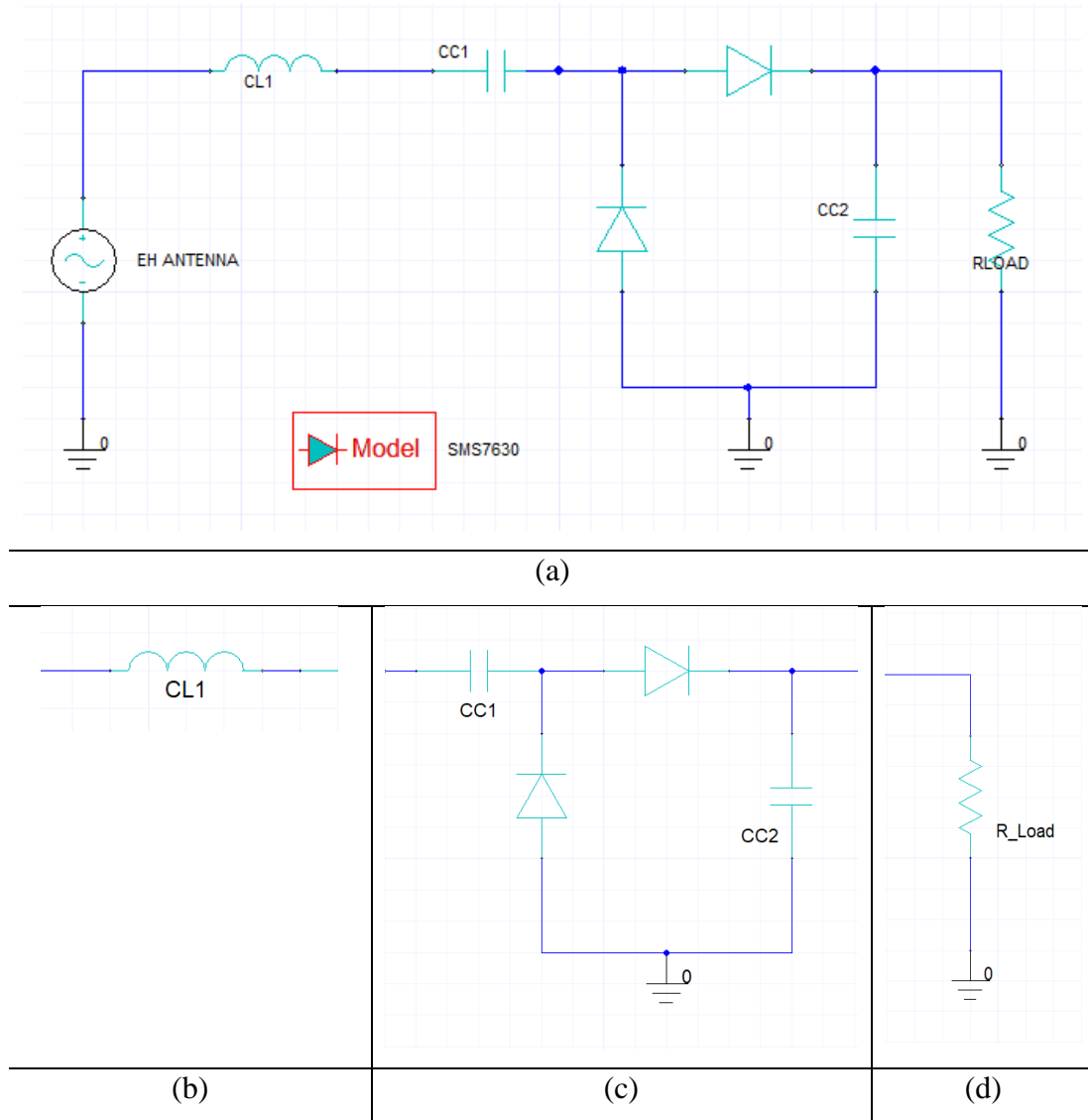


Figure 3.5 : (a) Configuration of the proposed RF energy harvesting system (antenna, matching circuit, rectifying circuit, and DC load), (b) matching element (circuit) (c) Villard voltage rectifier circuit, and (d) DC load.

In the harmonic balance analysis which performed in Ansys Electronics Desktop, the input impedance of one-stage voltage rectifier circuit has been obtained $29.8 - j272.1$ at -11 dBm input power value. The input impedance value has been set to $46 + j0.1$ using one inductor (CL1). The impedance matching between the antenna and the RF to DC rectification circuit is sufficient level, so the impedance matching circuit has been not designed, only the impedance matching element (one inductor) has been used. The impedance matching element (one inductor) is shown in Figure 3.5.b.

Rectifying circuit has been designed for obtaining DC output voltage from the gathered RF signal operates at 2400 MHz resonance frequency, which consisting of two diodes and two capacitors in a single stage Villard voltage rectifier topology have been composed. The Villard voltage rectifier circuit is shown in Figure 3.5.c.

The end of the impedance matching and RF to DC rectifier circuit is load resistance. After the design of the impedance matching and RF to DC rectifying circuit, the DC load value is determined as the most optimized value according to the input impedance and RF to DC conversion efficiency of this circuit. The DC load is shown in Figure 3.5.d.

In the RF to DC rectifying circuit, zero biased Schottky barrier diode SMS 7630 have been used. The Spice parameters of the SMS 7630 used the nonlinear simulation are presented in Table 3.3.

The lumped circuit element values of the impedance matching and RF to DC rectifying circuit with DC Load are listed in Table 3.5.

Table 3.5 : Design parameters of proposed impedance matching and RF to DC rectifying circuit with DC load.

CL1	CC1	CC2	Optimize R_load
21.7 nH	2 pF	10 pF	15 K Ω

4. NUMERICAL AND EXPERIMENTAL RESULTS

The performance parameters of designed Rectenna Design – 1 operates at 900 MHz and Rectenna Design – 2 operates at 2400 MHz have been presented in this section. Measurement and simulation studies of RF energy harvesting antennas and simulation studies of the impedance matching and RF to DC rectifying circuits have been conducted.

4.1 Rectenna Design – 1

The performance analysis of the components of the RF energy harvesting system has been performed. The electromagnetic performance parameters of the proposed energy harvesting antenna are numerically calculated in CST Studio Suite. The input reflection coefficient of the fabricated energy harvesting antenna prototype is measured by the SignalHound USB-SA124B Spectrum Analyzer and the USB-TG124A Monitoring Generator. The numerically calculated and experimental results of the input reflection coefficient (S_{11}) are shown in Figure 4.1.

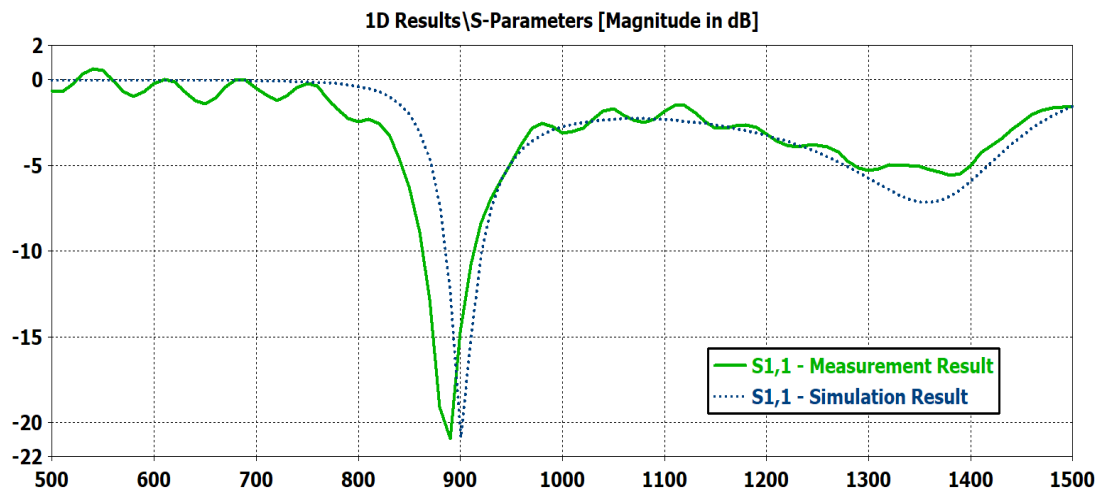
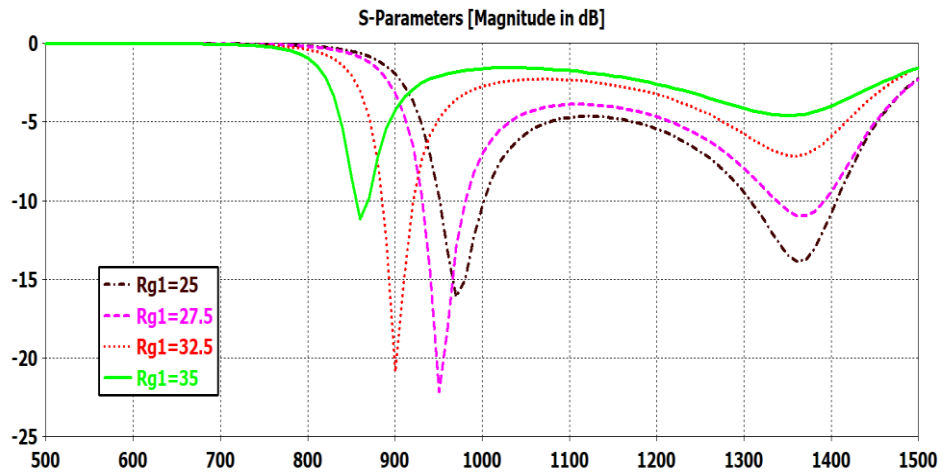


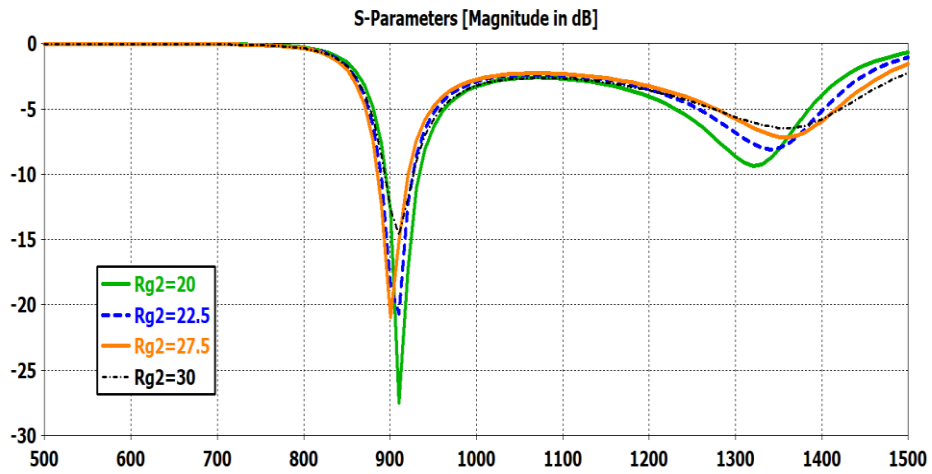
Figure 4.1 : The input reflection coefficient (S_{11}) of the modeled in CST and fabricated energy harvesting antenna.

The energy harvesting antenna, which is the component of the RF energy harvesting system, is designed to operate in the GSM 900 band by adjusting with geometric parameters. The numerically computed resonance frequency is 900 MHz with the return loss of 21 dB and 10 dB bandwidth of 34.6 MHz. The measured resonance frequency of the fabricated prototype is 890 MHz with the return loss of 21 dB and 10 dB bandwidth of 51.3 MHz. Although there are differences between the numerically computed and measured the resonance frequency, the width of the operating bandwidth is very close and similar, and the desired operating band performances have been obtained in both the modeled in CST and fabricated energy harvesting antenna.

Two essential parameters have been determined for shifting the resonance frequency to the desired frequency point and increasing the operation bandwidth. These parameters are the radius of the elliptical structure of the antenna design on the ground surface R_{g1} and R_{g2} . The R_{g1} parameter is effective in changing (shifting) the resonance frequency while the R_{g2} parameter is valid on the operation bandwidth. The effect of the R_{g1} and R_{g2} parametric study on the input reflection coefficient performance parameter is presented in Figure 4.2. All other parameters have been kept constant while performing parametric studies. However, when adjusting the resonance frequency and the operating bandwidth, it is necessary to conduct a parametric study with all parameters, including these two dominant parameters. By changing the parameters R_{g1} and R_{g2} , the perimeter of the elliptical structure on the ground surface changes, keeping the changing length below the critical value prevents the formation of a second resonance frequency and the evolution of the operating bandwidth which may occur from near-field radiation. However, when adjusting the resonance frequency and the operating bandwidth, it is necessary to conduct a parametric study with all parameters, including these two dominant parameters.



(a)



(b)

Figure 4.2 : The input reflection coefficient (S_{11}) of the proposed energy harvesting antenna with the different variables; (a) R_{g1} is variable (others are constant) and (b) R_{g2} is variable (others are constant).

The surface current distribution at the resonance frequency indicates the operating principle of the antenna. The surface current distributions of the energy harvesting antenna surface at resonance frequency 900 MHz are presented in Figure 4.3. When the surface current distribution of both surfaces of the antenna is examined, the λ resonance characteristics feature is observed. The resonance current distribution indicates the operation principle of the antenna. In the form of the λ resonance characteristic of split ring resonators capacitively coupling on the upper surface of the

antenna and in the form of electrical coupling between the slotted ground plane the bottom surface of the antenna.

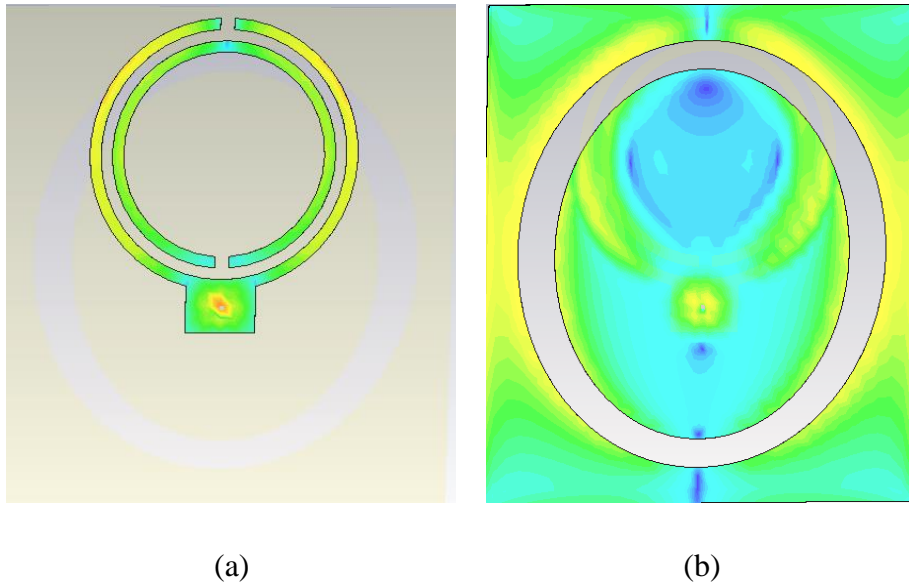
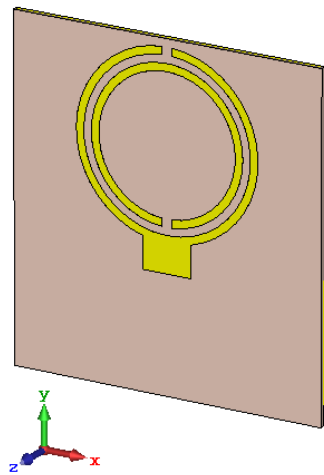


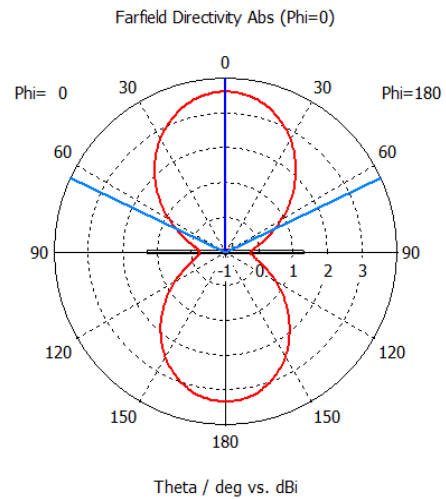
Figure 4.3 : The surface current distributions of the energy harvesting antenna at the resonance frequency; (a) top and (b) bottom views.

The 2D polar radiation patterns of energy harvesting antenna in free-space on X-Y, X-Z, and Y-Z planes at the resonance frequency 900 MHz are shown in Figure 4.4.

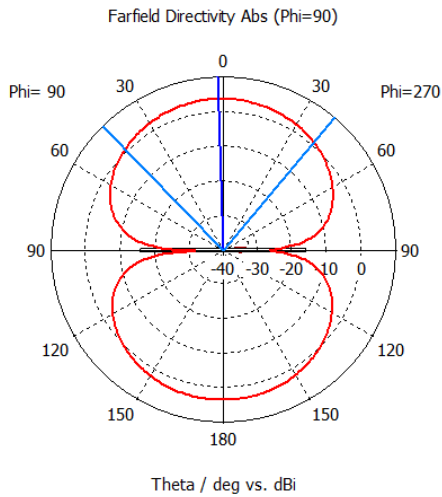
The half-power beamwidth (HPBW) is more than 90 degrees (94.8 degrees) in azimuth (X-Y) plane. When the 2D radiation pattern of the antenna is investigated, a directional antenna behavior is observed in the phi and theta planes.



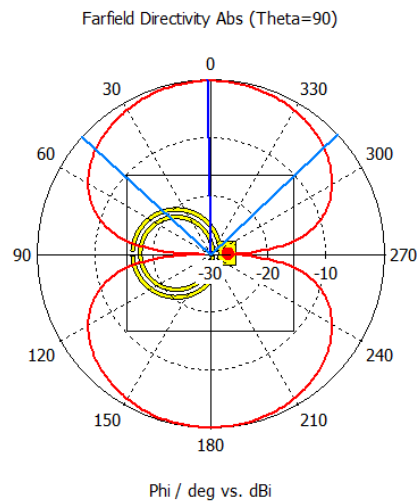
(a)



(b)



(c)



(d)

Figure 4.4 : The 2D (polar plot) radiation patterns of the energy harvesting antenna at the resonance frequency 900 MHz: (a) antenna design with coordinate system for demonstration of planes (b) X-Y plane, (c) X-Z plane, and (d) Y-Z plane.

The RF energy harvesting antenna has been designed to be as omnidirectional as possible so that it can gather the RF signals in all directions. The 3D radiation pattern of the proposed antenna is shown in Figure 4.5. The simulated peak gain has been obtained as 3.4 dBi at resonance frequency 900 MHz. The antenna radiation efficiency is 96.3% with the directivity of 3.61 dBi.

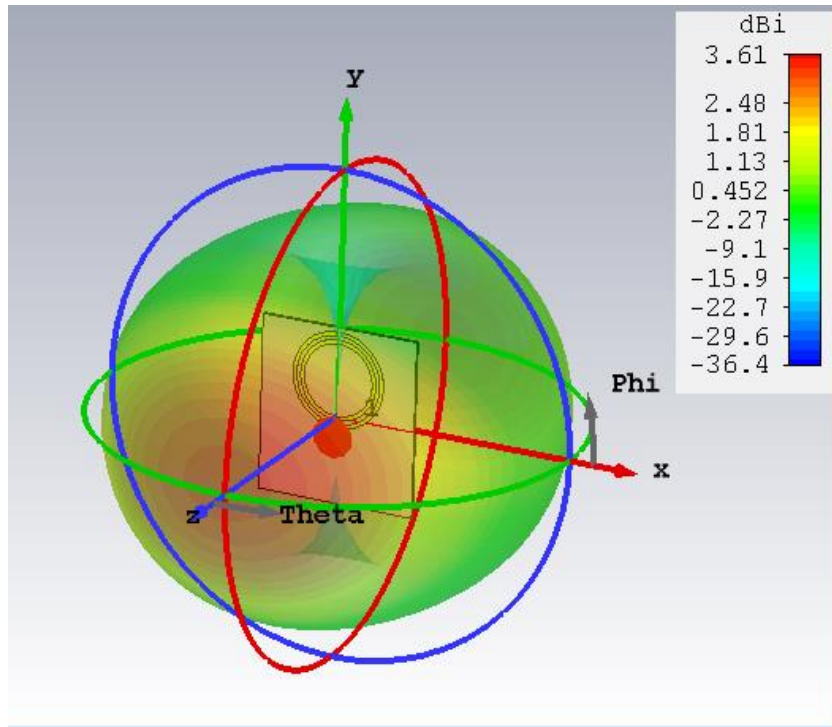


Figure 4.5 : The 3D radiation pattern of the proposed energy harvesting antenna at the resonance frequency of 900 MHz.

The RF energy harvesting performance of the antenna is numerically calculated to determine how much input RF signal value can be gathered in the receiving mode, as shown in the experimental setup model in Figure 4.6. To model this experimental setup in CST, the antenna feeding port is replaced by the lumped element (50 ohms resistance) as the port termination.

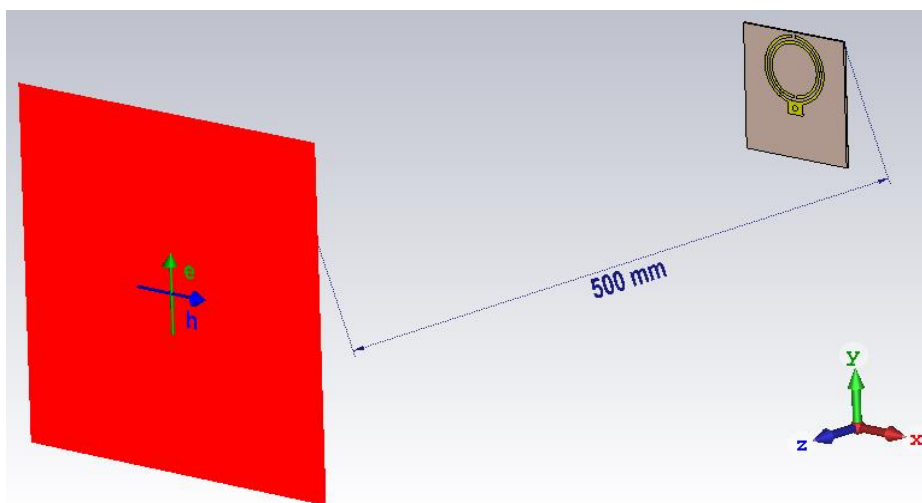
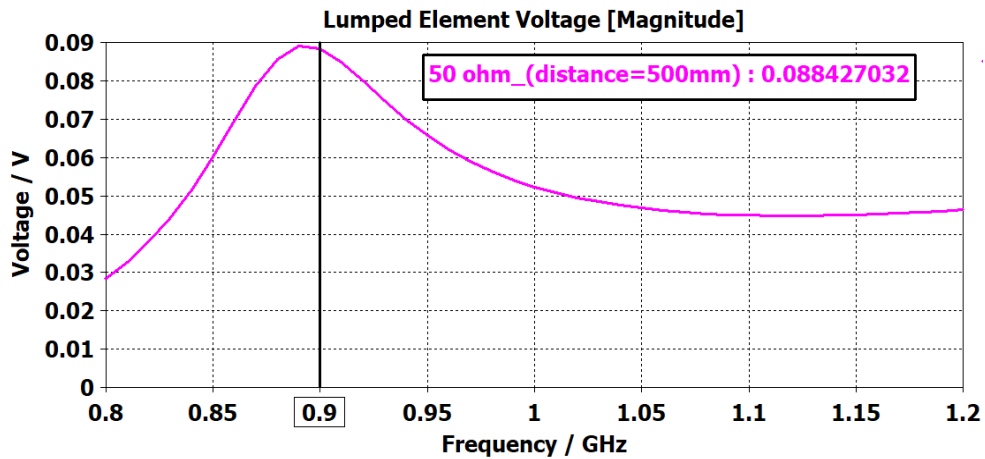
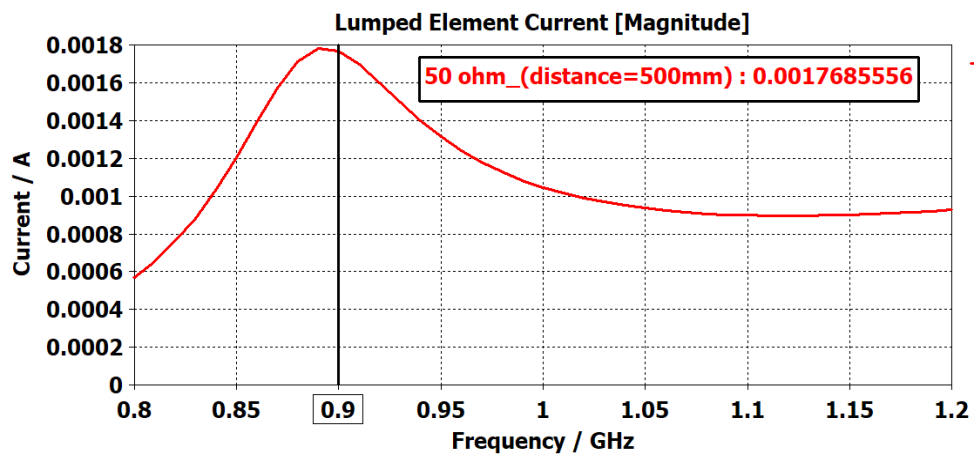


Figure 4.6 : RF energy harvesting antenna input power measurement setup.

The ambient radiating field is modeled as the plane wave excitation (1 Volt/m) experimental setup in a far-field region with a distance of 500 mm from the antenna. At the 900 MHz resonance frequency, the lumped element voltage of 88.42 mV (Figure 4.7.a) and current of 1.768 mA (Figure 4.7.b) are achieved which indicates the approximately -11 dBm (0.079 mW) power to be gathered by the receiving antenna. The terminal voltage and current values are shown in Figure 4.7.



(a)



(b)

Figure 4.7 : Terminal (a) voltage and (b) current values on the lumped element (antenna feeding port).

The RF to DC rectification performance of the proposed RF energy harvesting system operating at 900 MHz has been obtained with the numerical evaluations in the commercially available radio frequency electronic circuit design software, Ansoft Designer.

The input reflection coefficient of the impedance matching and RF to DC rectifying circuit is obtained by applying different input RF power values to the circuit input (from the antenna). The input reflection coefficient of the RF energy harvesting system at the resonance frequency 900 MHz is shown in Figure 4.8. The input impedance of the impedance matching and RF to DC rectifying circuit has a maximum matching 50 Ω antenna input impedance in the 900 MHz at the RF input power level of -30 dBm. As the system shows a nonlinear characteristic, different input reflection coefficient values are obtained with different input RF power values.

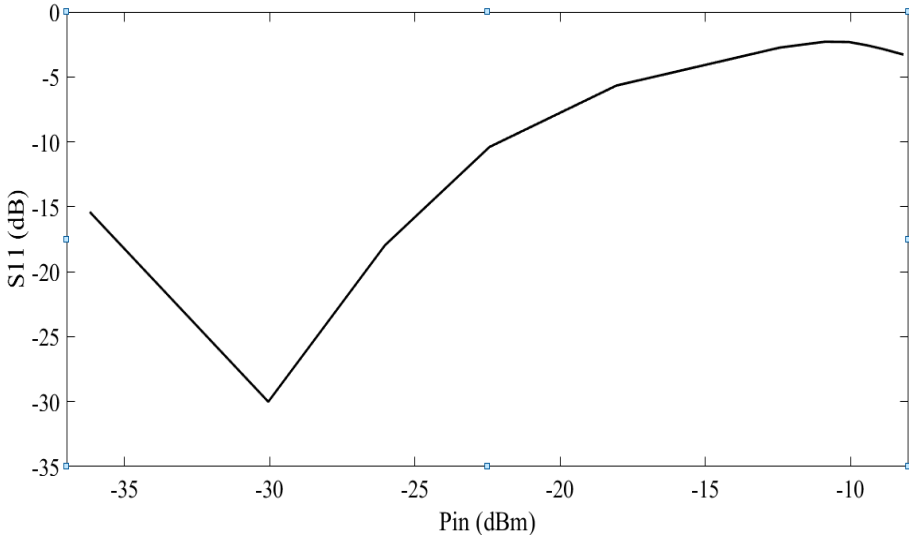


Figure 4.8 : The input reflection coefficient of the RF energy harvesting system at the resonance frequency with different RF input values.

The RF to DC conversion efficiency of the RF energy harvesting system is obtained by applying different input RF power values to the RF to DC rectifying circuit input. The RF to DC conversion efficiency of the RF energy harvesting system at the resonance frequency is shown in Figure 4.9. The best RF to DC conversion efficiency is observed with the maximum value of 75% for the input power level of -11 dBm at the resonance frequency 900 MHz.

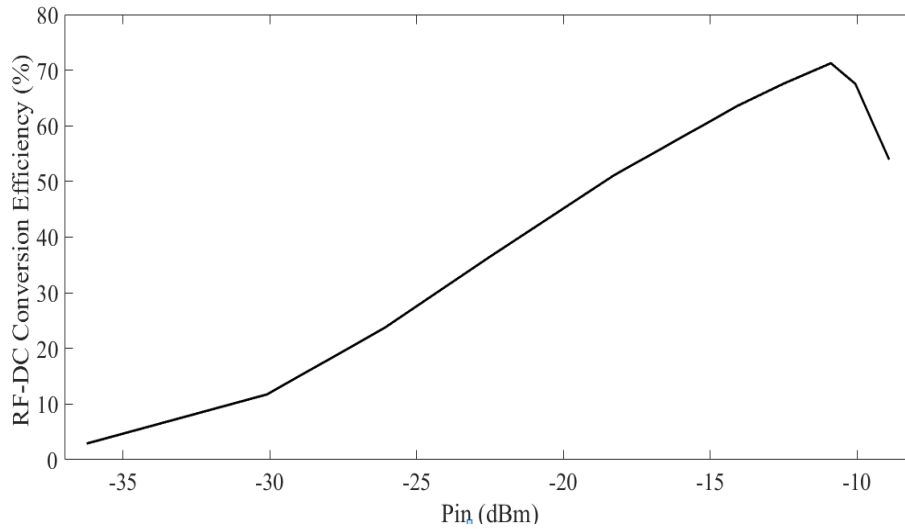


Figure 4.9 : The RF to DC conversion efficiency of the impedance matching and RF to DC rectifying circuit at the resonance frequency with different RF input values.

Another one of the critical success parameters of RF energy harvesting systems is the high output DC voltage. The DC output voltage value of these systems intends to be as high as possible. The output DC voltage values of the RF energy harvesting system is obtained by applying different input RF power values to the RF to DC rectifying circuit input. The output DC voltage values of the RF energy harvesting system at the resonance frequency is shown in Figure 4.10. The output DC voltage is observed with a value of 1.7 V for the input power level of -11 dBm at the resonance frequency 900 MHz.

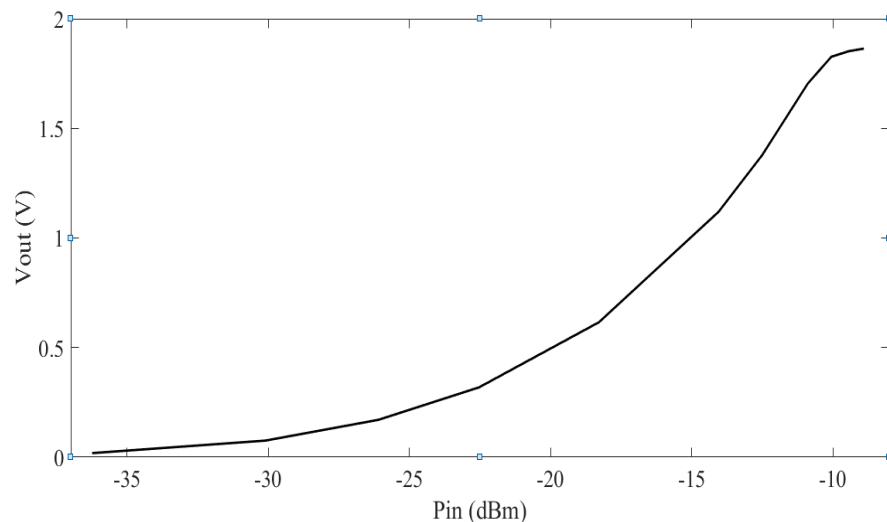


Figure 4.10 : The output DC voltage values of the impedance matching and RF to DC rectifying circuit at the resonance frequency with different RF input values.

It is directly related to the output DC voltage of the DC load resistor. The effect of the DC load resistance on the output DC voltage is shown in Figure 4.11. As a result of input impedance mismatch of the impedance matching and RF to DC rectifying circuit and power distribution in the generated higher order harmonics in the Schottky barrier diodes for different DC load resistances, the output voltage is not increased proportionally to DC load resistances.

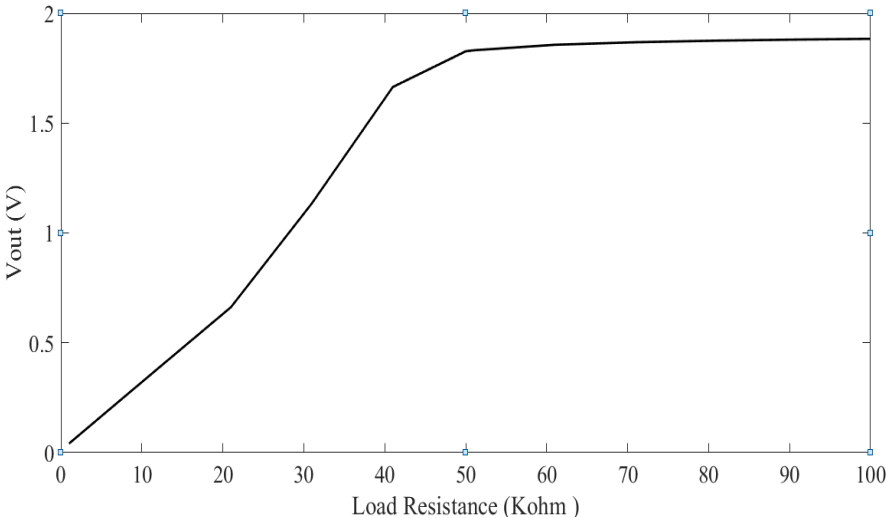


Figure 4.11 : The DC output voltage level of the impedance matching and RF to DC rectifying circuit at the resonance frequency with different DC load resistance.

However, the maximum RF to DC conversion efficiency of 75% has been obtained at -11 dBm input power level for the impedance matching and RF to DC rectifying circuit. To demonstrate the time domain rectification feature of impedance matching and RF to DC rectifying circuit, the input RF signal and output DC voltage for -11 dBm input power are shown in Figure 4.12. The input RF signal amplitude and output DC voltage value are 28 mV and 1.7 V, respectively.

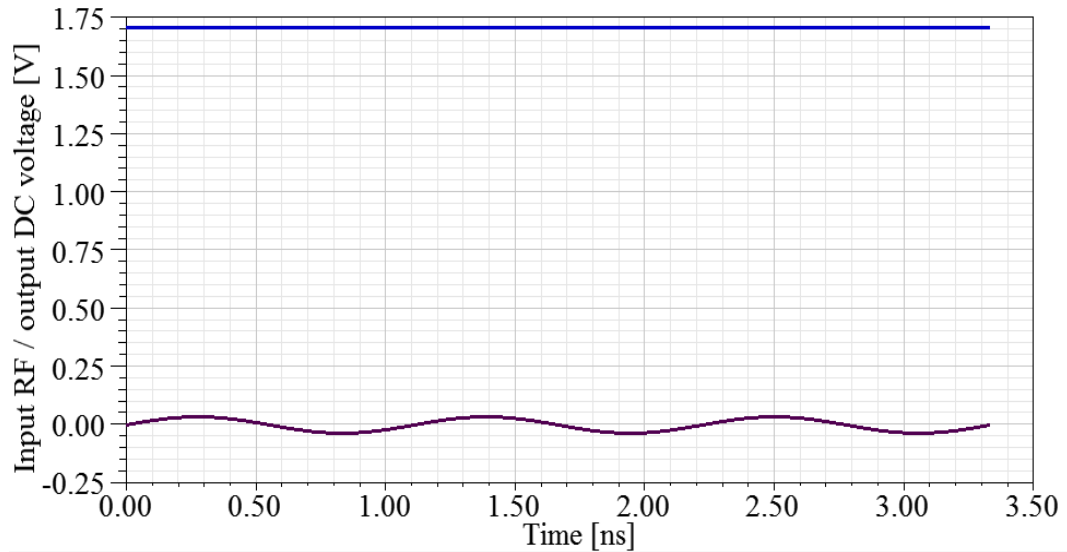


Figure 4.12 : RF input and output DC voltage values of the proposed impedance matching and RF to DC rectifying circuit for -11dBm input RF power.

Rectenna Design – 1 consisting of a probe-fed split ring resonator on the elliptical slotted ground plane in conjunction with impedance matching and RF to DC rectifying circuit is proposed and numerically investigated for the energy harvesting applications at 900 MHz. The nonlinear modeling and systematic optimization of the proposed rectenna have been performed as a whole complete system. The numerical and experimental results indicate the proposed rectenna to generate 1.7 V DC output voltage at the center frequency of 900 MHz for -11 dBm input power. The rectenna design numerically calculated performance parameters shown in Table 4.1.

Table 4.1 : Rectenna Design – 1 simulated performance parameters.

Antenna Gain	Antenna Radiation Efficiency	Antenna Total Efficiency
3.42 dBi	96.3 %	93.4 %
Antenna Directivity	Antenna Operating Frequency	Antenna Resonance Frequency
3.61 dBi	885 – 920.6 MHz	900 MHz
Antenna Bandwidth	System RF to DC Conversion Efficiency	System Output Voltage
34.6 MHz	-11 dBm: 75%	-11 dBm: 1.7 V

4.2 Rectenna Design – 2

The performance analysis of the components of the Rectenna Design – 2 (RF energy harvesting system) has been performed. The electromagnetic performance parameters of the proposed energy harvesting antenna are numerically calculated in CST Studio Suite. The input reflection coefficient of the fabricated energy harvesting antenna prototype is measured by the SignalHound USB-SA124B Spectrum Analyzer and the USB-TG124A Monitoring Generator. The numerically calculated and experimental results of the input reflection coefficient (S_{11}) are shown in Figure 4.13.

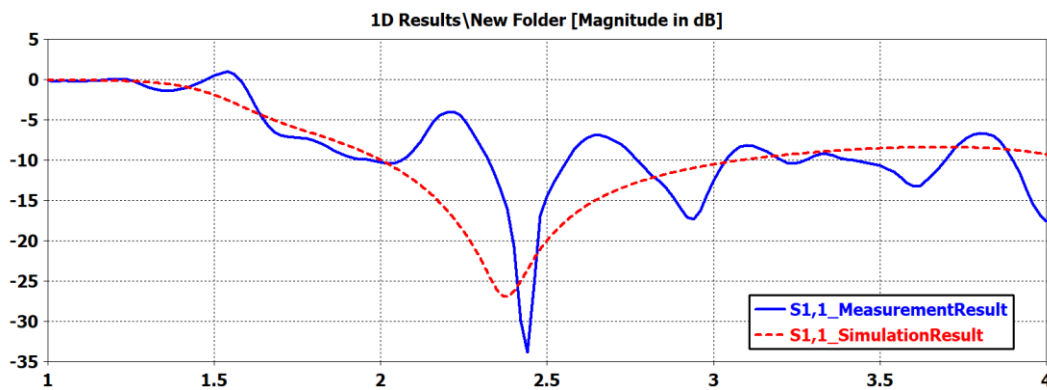
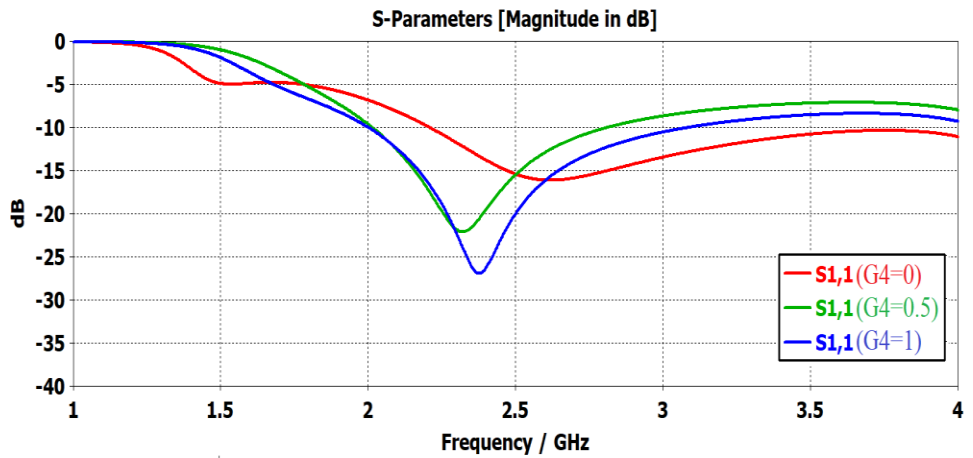


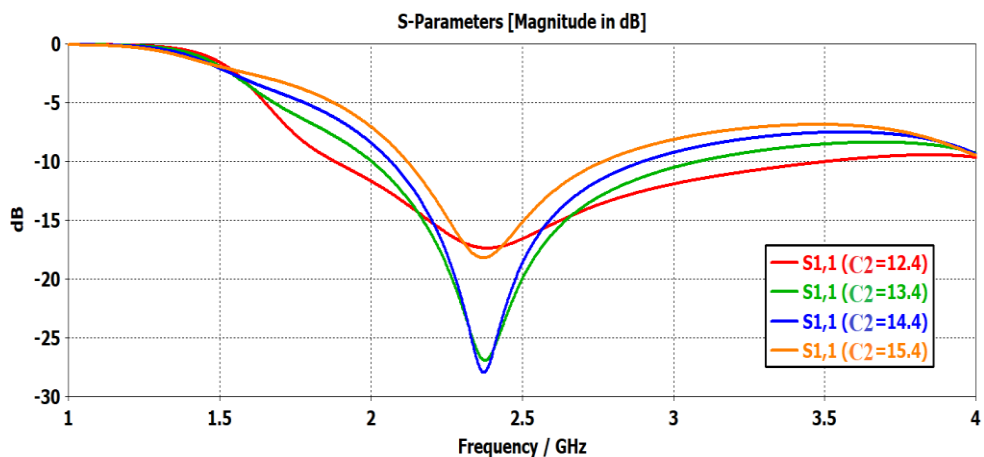
Figure 4.13 : The input reflection coefficient (S_{11}) of the modeled in CST and fabricated energy harvesting antenna.

The energy harvesting antenna, which is the component of the RF energy harvesting system, is designed to operate in the ISM 2.4 GHz band by adjusting with geometric parameters. The numerically computed resonance frequency is 2.38 GHz with the return loss of 27 dB and 10 dB bandwidth of 1050 MHz. The resonance frequency of the fabricated prototype is 2.44 GHz with the return loss of 34 dB and 10 dB bandwidth of 240 MHz. Numerical computations are done for the optimization of the proposed energy harvesting antenna to have the resonance frequency at 2.44 GHz. There are some differences between the input reflection coefficient simulation and measurement results. The reason for these differences is thought to be because the antenna could not be produced with the desired precision (the length of G4 on the fabricated prototype has occurred in the same path at different heights). However, despite these differences, the input reflection coefficient measurement and simulation results prove very similar characteristics.

The antenna design parameters have been optimized in that the proposed energy harvesting antenna has a resonant frequency at 2.4 GHz and wide operating bandwidth. According to the optimization studies which is performed in the simulation environment, the most critical parameters affecting the resonance frequency and operating bandwidth are G4 on the bottom layer and C2 on the top layer. The results of the input reflection coefficient, which are indicated the effect of G4 and C2 parameters on the resonance frequency and the operating bandwidth are presented in Figure 4.14. Although the G4 parameter does not seem to be of great importance in antenna operation, the antenna has a considerable influence on the operation bandwidth and the resonance frequency (Figure 4.14.a).



(a)



(b)

Figure 4.14 : The input reflection coefficient (S_{11}) of the proposed energy harvesting antenna with the different variables; (a) G4 parameter is variable (others are constant), and (b) C2 parameter is variable (others are constant).

The parameter C2 has no effect on the resonance frequency, but has a significant impact on the operating bandwidth and is optimized to provide maximum bandwidth as a result of the parametric study (Figure 4.14.b).

The surface current distribution at of 2.4 GHz is shown in Figure 4.15. The current distribution indicates the operation principle of the antenna. The antenna operation principle relies on the resonant excitation of mainly capacitively coupled directly fed fork-shaped resonator to the parasitic T shaped resonator in conjunction with the rectangular slot resonator in the ground plane.

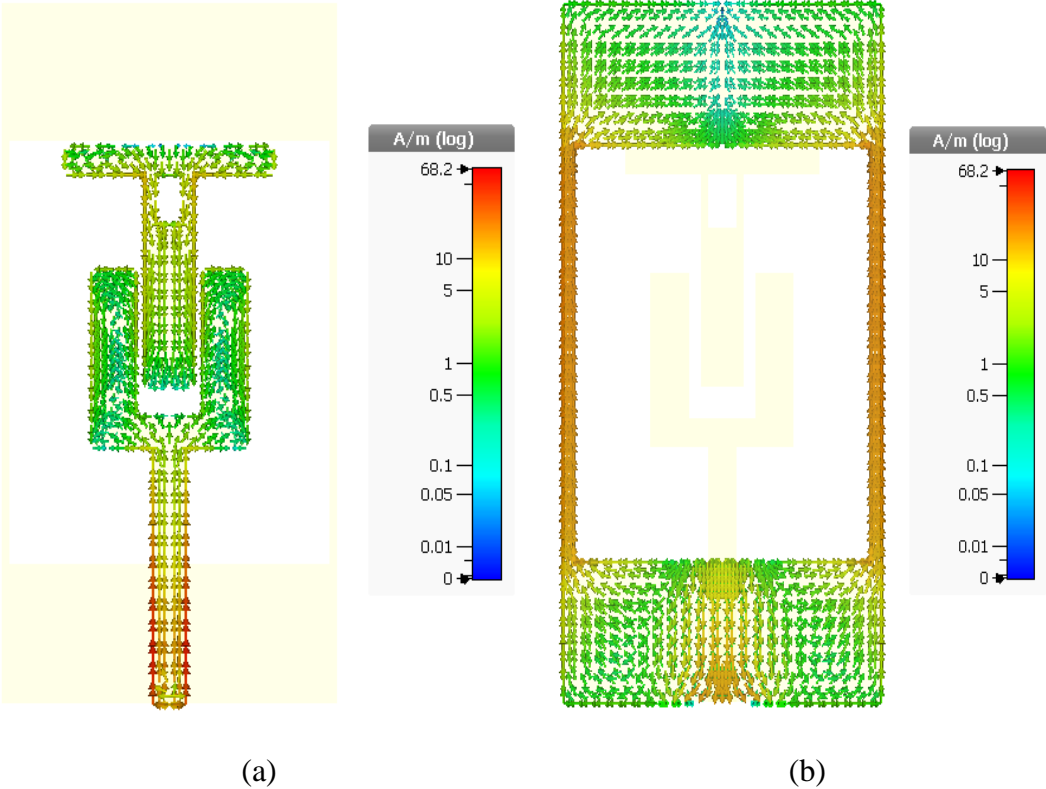


Figure 4.15 : The surface current distribution of the proposed energy harvesting antenna; (a) top and (b) bottom layers.

The 2D polar radiation patterns of energy harvesting antenna on X-Z ($\phi=0$), Y-Z ($\phi=90$), and X-Y ($\theta=90$) planes are shown in Figure 4.16. The half power beam width (HPBW) is 80.8 degrees in Y-Z plane. The numerically computed realized gain is 2.4 dBi at the resonance frequency in the operating frequency band. The antenna

radiation efficiency is computed to be 98.9% with the total efficiency of 96.3% with the directivity of 2.57 dBi.

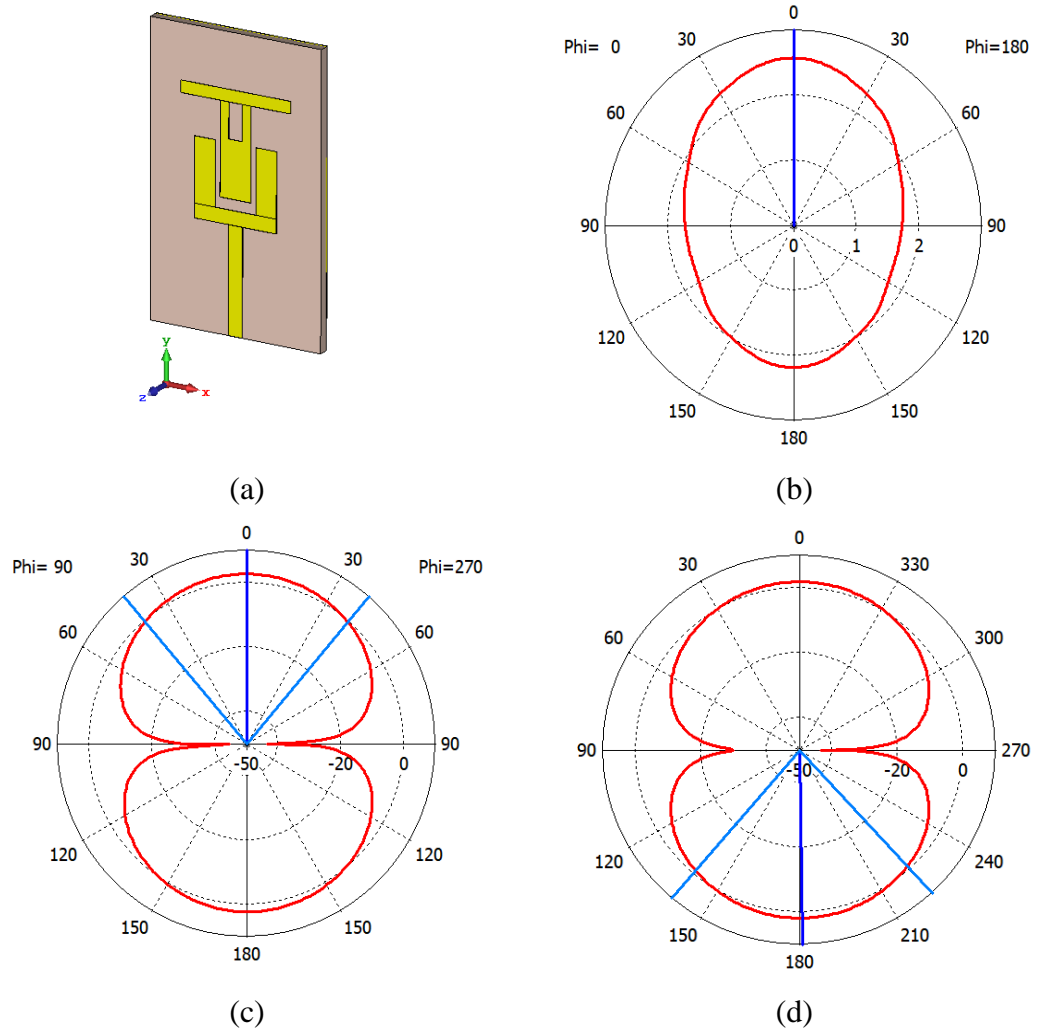


Figure 4.16 : The 2D (polar plot) radiation patterns of the energy harvesting antenna at the resonance frequency 2.4 GHz: (a) antenna design with coordinate system for demonstration of planes (b) X-Y plane, (c) X-Z plane, and (d) Y-Z plane.

The 3D radiation pattern of the proposed antenna is shown in Figure 4.17. The simulated peak gain has been obtained as 2.27 dBi at resonance frequency 2400 MHz. The antenna radiation efficiency is 99.57% with the directivity of 2.62 dBi.

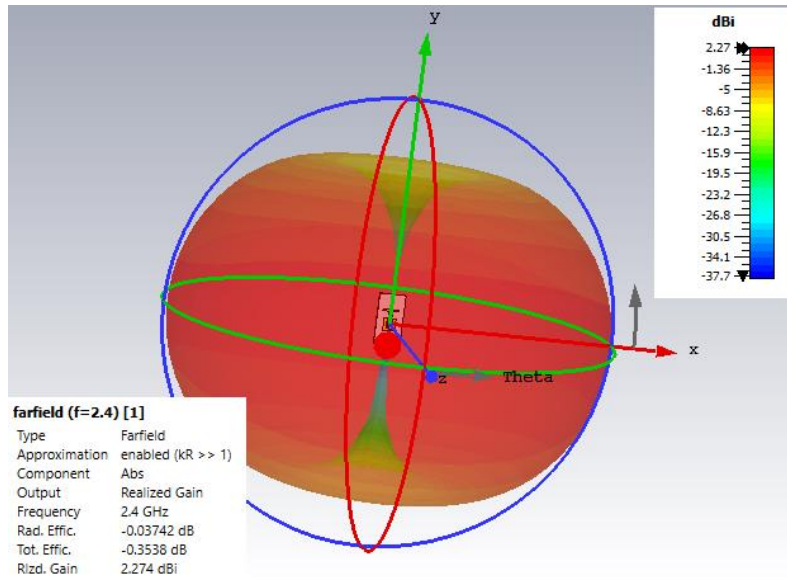


Figure 4.17 : The 3D radiation pattern of the proposed energy harvesting antenna at the resonance frequency of 2.4 GHz.

The experimental setup in Figure 4.18 has been built in the simulation environment to examining the RF signal gathering performance of the energy harvesting antenna. The antenna feeding port is replaced with a 50 ohm lumped element to set up the experimental setup, and this antenna is applied to the plane wave source located in the far-field region of the antenna (40 mm).

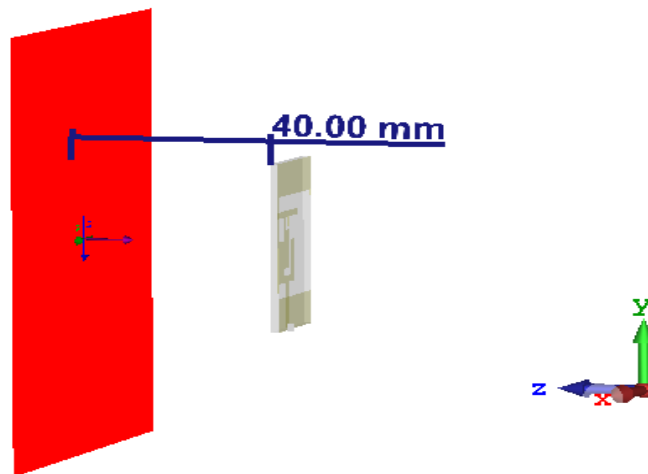
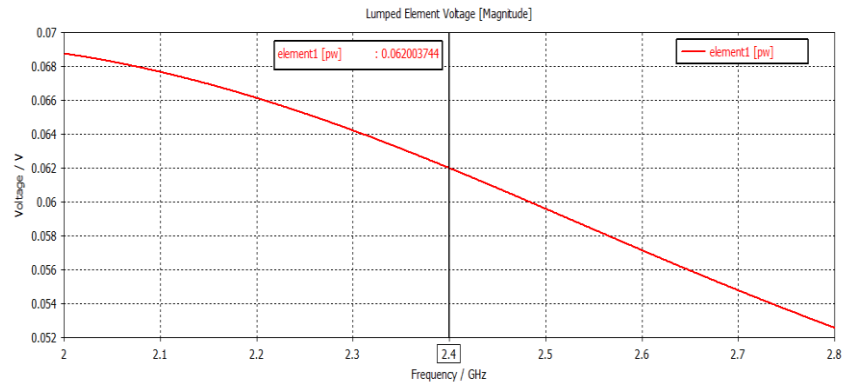


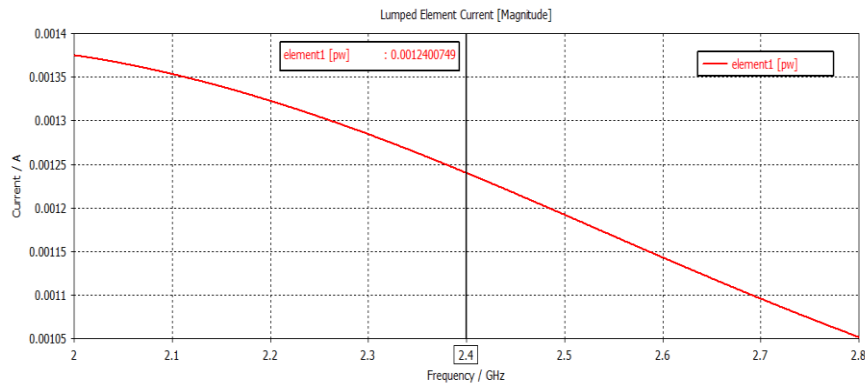
Figure 4.18 : Energy harvesting antenna input power measurement setup.

When an electric field is applied from the plane wave source to the energy harvesting antenna, on the lumped element (50 ohms resistance) is gathered 62 mV voltage

(Figure 4.19.a) and 1.24 mA current (Figure 4.19.b) as presented in Figure 4.19 at the 2.4 GHz (-11 dBm).



(a)



(b)

Figure 4.19 : (a) Voltage and (b) current values on the lumped element (antenna feeding port).

The RF to DC rectification performance of the proposed RF energy harvesting system operating at 2400 Mhz has been obtained with the numerical evaluations in the commercially available radio frequency electronic circuit design software, Ansoft Electronics Desktop.

The input reflection coefficient of the impedance matching and RF to DC rectifying circuit is obtained by applying different input RF power values to the circuit input (from the antenna). The input reflection coefficient of the RF energy harvesting system at the resonance frequency 2400 MHz is shown in Figure 4.20. The input impedance of the impedance matching and RF to DC rectifying circuit has a maximum matching

50 Ω antenna input impedance in the 2400 MHz at the RF input power level of -11 dBm. As the system shows a nonlinear characteristic, different input reflection coefficient values are obtained with different input RF power values.

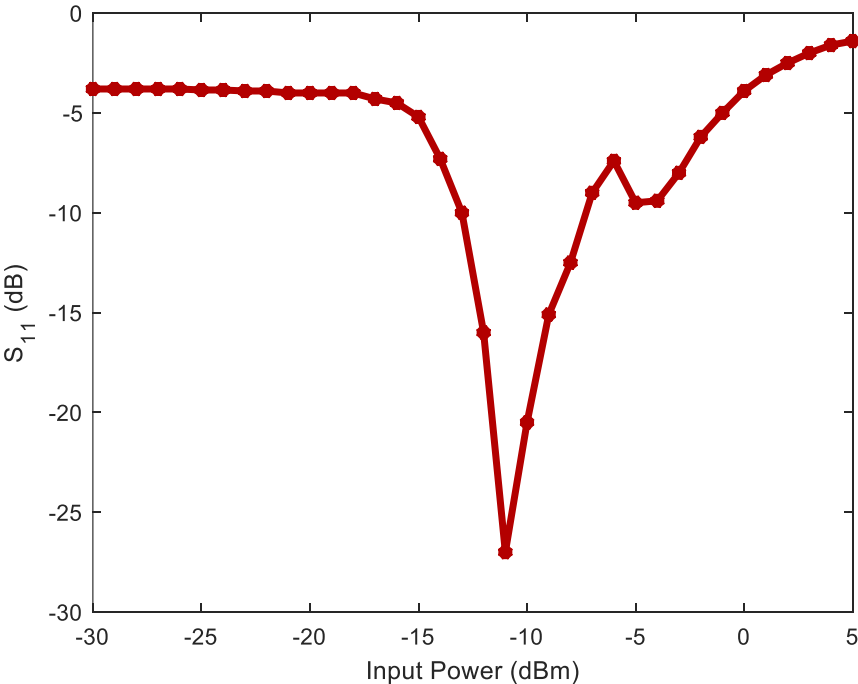


Figure 4.20 : The input reflection coefficient of the RF energy harvesting system at the resonance frequency with different RF input values.

The RF to DC conversion efficiency of the RF energy harvesting system is obtained by applying different input RF power values to the RF to DC rectifying circuit input. The RF to DC conversion efficiency of the RF energy harvesting system at the resonance frequency is shown in Figure 4.21. The best RF to DC conversion efficiency is observed with the maximum value of 79.3 % for the input power level of -6 dBm at the resonance frequency 2400 MHz. Also, 49 % RF to DC conversion efficiency is observed for the input power level of -11 dBm.

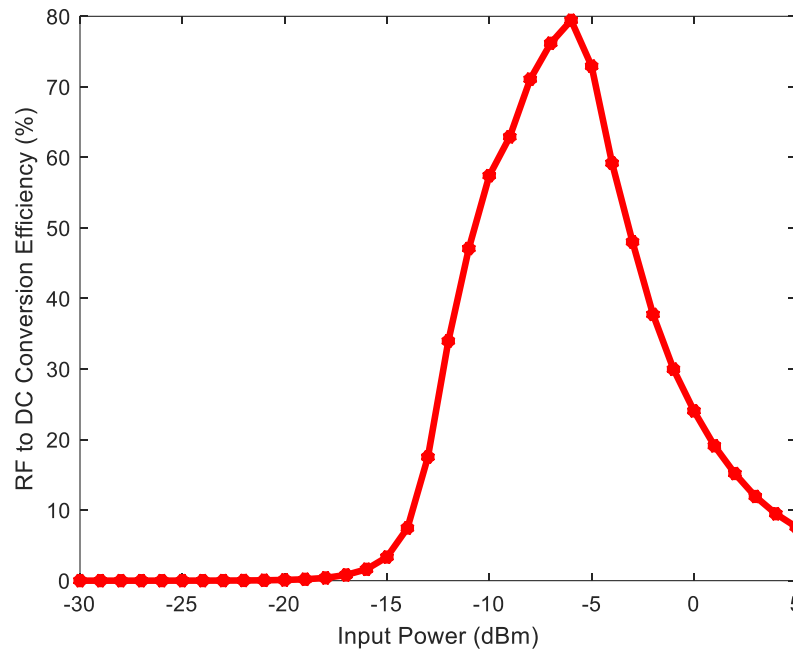


Figure 4.21 : The RF to DC conversion efficiency of the impedance matching and RF to DC rectifying circuit at the resonance frequency with different RF input values.

Another one of the vital success parameters of RF energy harvesting systems is the high output DC voltage. The output DC voltage values of the RF energy harvesting system is obtained by applying different input RF power values to the RF to DC rectifying circuit input. The output DC voltage values of the RF energy harvesting system at the resonance frequency is shown in Figure 4.22. The output DC voltage is observed with a value of 0.75 V for the input power level of -11 dBm at the resonance frequency 2400 MHz. Also, 1.73 V output DC voltage is observed for the input power level of -6 dBm (at the best RF to DC conversion efficiency point).

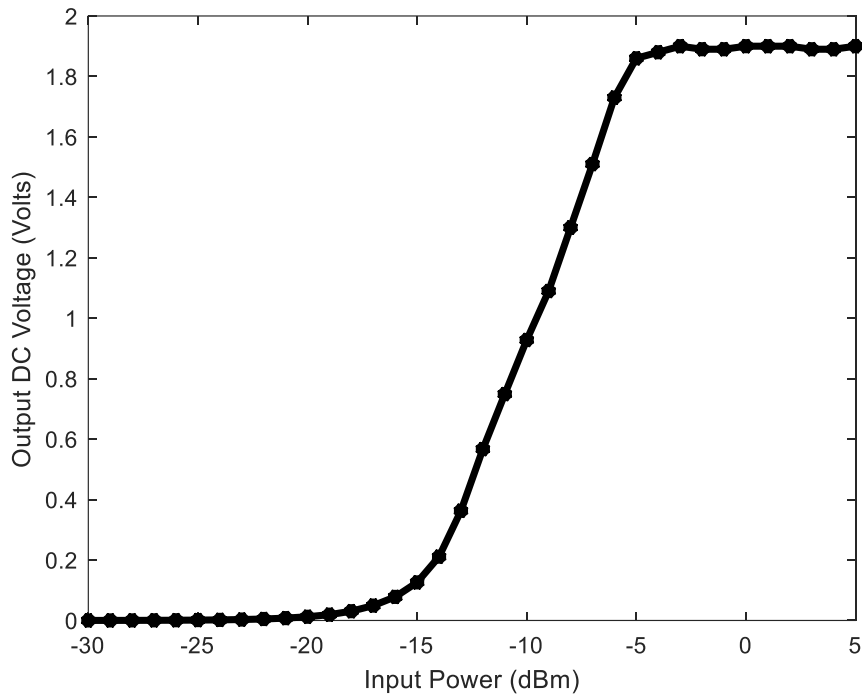


Figure 4.22 : The output DC voltage values of the impedance matching and RF to DC rectifying circuit at the resonance frequency with different RF input values.

The effect of the DC load resistance on the output DC voltage is shown in Figure 4.23.

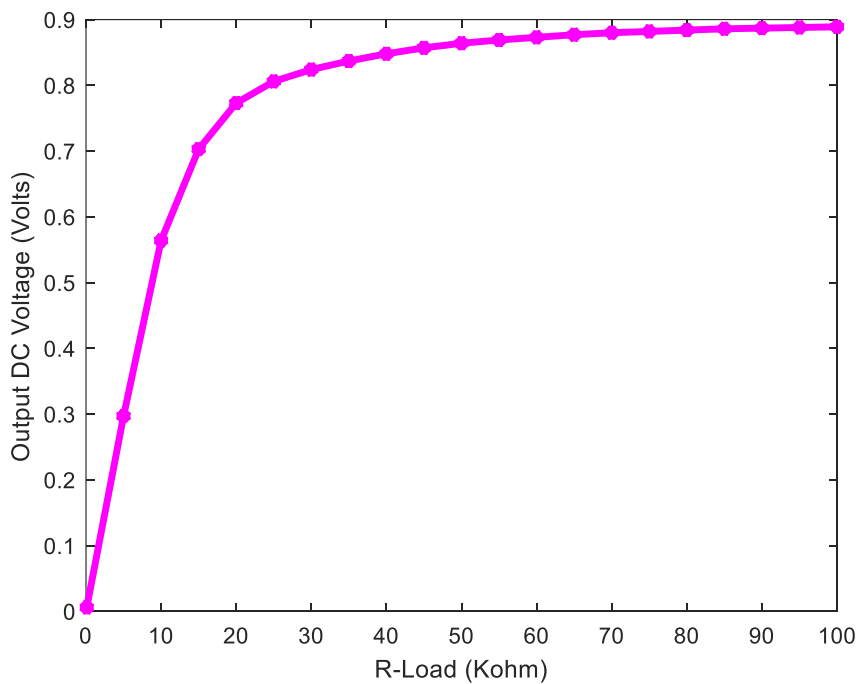


Figure 4.23 : The DC output voltage level of the impedance matching and RF to DC rectifying circuit at the resonance frequency with different DC load resistance.

The effect of the DC load resistance on the RF to DC conversion efficiency is shown in Figure 4.24.

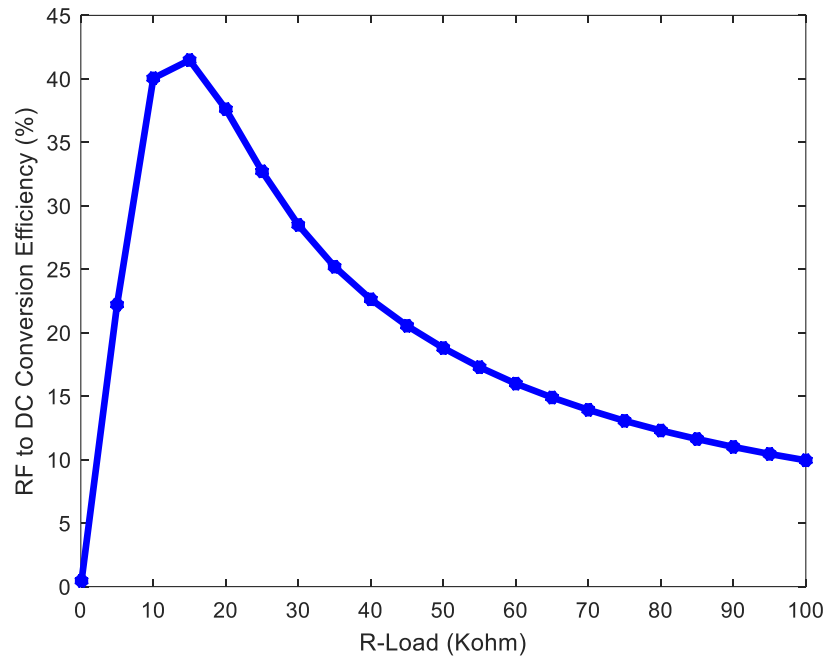


Figure 4.24 : The RF to DC conversion efficiency of the impedance matching and RF to DC rectifying circuit at the resonance frequency with different DC load resistance.

The output DC voltage levels and RF to DC conversion efficiency have been investigated at variable output DC load resistance values. After this investigation, the optimum load resistance value has been determined to be 15 K Ω at 2400 MHz resonance frequency with -11 dBm input.

However, the maximum RF to DC conversion efficiency of 49% has been obtained at -11 dBm input power level for the impedance matching and RF to DC rectifying circuit. To demonstrate the time domain rectification feature of impedance matching and RF to DC rectifying circuit, the input RF signal (V_{in}) and output DC voltage (V_{out}) for -11 dBm input power is shown in Figure 4.25. The signal obtained after impedance matching (V_{in1}) is presented in the same figure. The input RF signal amplitude and output DC voltage value are 28 mV and 0.75 V, respectively.

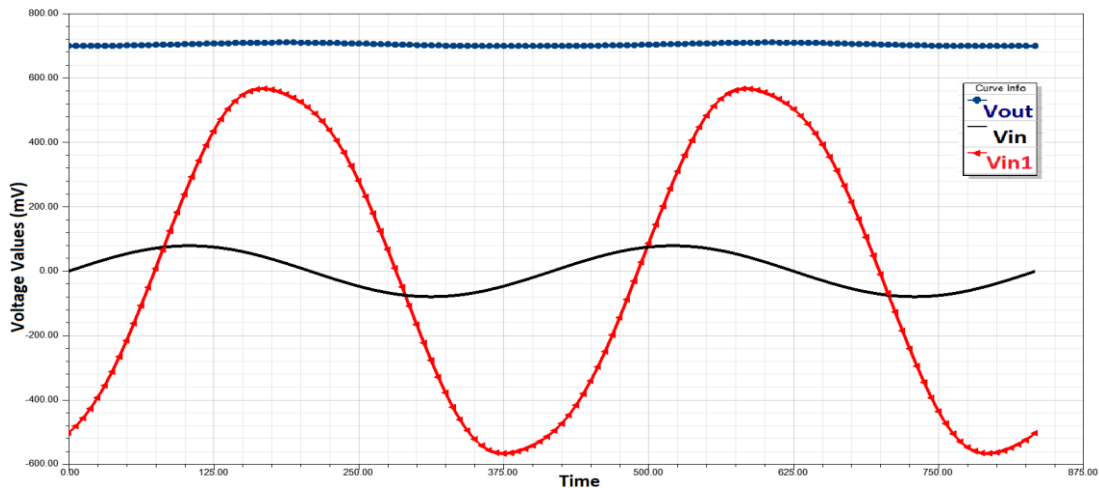


Figure 4.25 : RF input and output DC voltage values of the proposed impedance matching and RF to DC rectifying circuit for -11dBm input RF power (Vin – Input RF signal (from the antenna), Vin1 – RF to DC rectifying circuit input signal (after matching), and Vout – Output DC voltage).

Rectenna Design – 2 consisting of RF energy harvesting antenna with impedance matching and RF to DC rectifying circuit is proposed and numerically investigated for the energy harvesting applications at 2400 MHz. The nonlinear modeling and systematic optimization of the proposed rectenna have been performed as a whole complete system. The numerical and experimental results indicate the proposed rectenna to generate 0.75 V output DC voltage at the center frequency of 2400 MHz for -11 dBm input power. The rectenna design numerically calculated performance parameters shown in Table 4.2.

Table 4.2 : Rectenna Design – 2 simulated performance parameters.

Antenna Gain	Antenna Radiation Efficiency	Antenna Total Efficiency
2.27 dBi	99.57 %	99.3 %
Antenna Directivity	Antenna Operating Frequency	Antenna Resonance Frequency
2.62 dBi	2.05 – 3.1 GHz	2.38 GHz
Antenna Bandwidth	System RF to DC Conversion Efficiency	System Output Voltage
1.05 GHz	-11 dBm: 49 %	-11 dBm: 0.75 V

5. CONCLUSION AND FUTURE WORK

5.1 Conclusion

With the rapid development of technology, a large number of wireless systems radiated electromagnetic energy into the environment. Most of this radiated energy is disappearing before reaching their target, and recycling ambient energy solution rectenna studies have aroused great attention, allowing to eliminate this problem efficiently.

This study aims to design two different RF energy harvesting system able to harvest ambient RF power existing in the GSM 900 MHz, and ISM 2.4 GHz bands. The focus of this study is on designing a highly efficient system at low input power (-11 dBm) capable of power a DC Load (low power devices).

The rectenna designs have been proposed and numerically investigated for RF energy harvesting applications. The parametric and systematic optimization of antennas and nonlinear modeling of the rectifying circuit designs have been performed as a whole complete rectenna system. In Rectenna Design – 1 consisting probe fed split ring resonator on the elliptical slotted ground plane in conjunction with impedance matching and RF to DC rectifying circuit (Villard voltage rectifier topology), numerical and experimental results indicate to generate 1.7 V output DC voltage (with % 75 RF to DC conversion efficiency) at the center frequency of 900 MHz for -11 dBm input power. In Rectenna Design – 2 consisting RF energy harvesting antenna with impedance matching and RF to DC rectifying circuit (Villard voltage rectifier topology), numerical and experimental results indicate to generate 0.75 V output DC voltage (with % 49 RF to DC conversion efficiency) at the center frequency of 2400 MHz for -11 dBm input power.

As a result, the proposed rectenna designs have been numerically and experimentally validated to meet the operational needs of low power devices.

5.2 Future Work

The future work related to this study will be the fabrication of the proposed rectenna systems and the measurement of output DC voltage.

The output DC voltage values can be increased sufficiently by several methods to operate any low power and low voltage electronic devices: Firstly, by increasing the number of the proposed antenna, it can be used in an antenna array, resulting in more input RF power. Secondly, the output DC voltage can be increased by using a multi-stage voltage rectifier circuit. However, when the multi-stage rectifier is used, advanced matching techniques must be applied to reduce the capacitive effect of the nonlinear circuit. Lastly, both the input RF power and output DC voltage can be increased by improving the design of the multi-band RF energy harvesting system.

REFERENCES

- [1] Chalasani, S., & Conrad, J. M. (2008). A survey of energy harvesting sources for embedded systems. *IEEE Southeast Con 2008*, 442–447. <https://doi.org/10.1109/SECON.2008.4494336>
- [2] Annapureddy, V., Palneedi, H., Hwang, G.-T., Peddigari, M., Jeong, D.-Y., Yoon, W.-H., Kim, K. H., & Ryu, J. (2017). Magnetic energy harvesting with magnetoelectrics: an emerging technology for self-powered autonomous systems. *Sustainable Energy & Fuels*, 1(10), 2039–2052. <https://doi.org/10.1039/C7SE00403F>
- [3] Lu, X., Wang, P., Niyato, D., Kim, D. I., & Han, Z. (2015). Wireless Networks With RF Energy Harvesting: A Contemporary Survey. *IEEE Communications Surveys & Tutorials*, 17(2), 757–789. <https://doi.org/10.1109/COMST.2014.2368999>
- [4] Saranya, N., & Kesavamurthy, T. (2019). Design and performance analysis of broadband rectenna for an efficient RF energy harvesting application. *International Journal of RF and Microwave Computer-Aided Engineering*, 29(1), e21628. <https://doi.org/10.1002/mmce.21628>
- [5] Kurs, A., Karalis, A., Moffatt, R., Joannopoulos, J. D., Fisher, P., & Soljačić, M. (2007). Wireless Power Transfer via Strongly Coupled Magnetic Resonances. *Science*, 317(5834), 83 LP-86. <https://doi.org/10.1126/science.1143254>
- [6] Mikeka, C. (2011). Design Issues in Radio Frequency Energy Harvesting System (H. A. E.-Y. K. Tan, Ed.). <https://doi.org/10.5772/25348>
- [7] Almonneef, T. S., Erkmen, F., Alotaibi, M. A., & Ramahi, O. M. (2018). A New Approach to Microwave Rectennas Using Tightly Coupled Antennas. *IEEE Transactions on Antennas and Propagation*, 66(4), 1714–1724. <https://doi.org/10.1109/TAP.2018.2806398>
- [8] Kimionis, J., Isakov, M., Koh, B. S., Georgiadis, A., & Tentzeris, M. M. (2015). 3D-Printed Origami Packaging With Inkjet-Printed Antennas for RF Harvesting Sensors. *IEEE Transactions on Microwave Theory and Techniques*, 63(12), 4521–4532. <https://doi.org/10.1109/TMTT.2015.2494580>
- [9] Kim, Y., Bhamra, H. S., Joseph, J., & Irazoqui, P. P. (2015). An Ultra-Low-Power RF Energy-Harvesting Transceiver for Multiple-Node Sensor Application. *IEEE Transactions on Circuits and Systems II: Express Briefs*, 62(11), 1028–1032. <https://doi.org/10.1109/TCSII.2015.2456511>
- [10] Uzun, Y. (2016). Design and Implementation of RF Energy Harvesting System for Low-Power Electronic Devices. *Journal of Electronic Materials*, 45(8), 3842–3847. <https://doi.org/10.1007/s11664-016-4441-5>

- [11] Jeong, J., & Jeong, Y. (2017). A novel dual-band RF energy harvesting circuit with power management unit for low power applications. *Microwave and Optical Technology Letters*, 59(8), 1808–1812. <https://doi.org/10.1002/mop.30630>
- [12] Gudan, K., Shao, S., Hull, J. J., Ensworth, J., & Reynolds, M. S. (2015). Ultra-low power 2.4GHz RF energy harvesting and storage system with -25dBm sensitivity. *2015 IEEE International Conference on RFID (RFID)*, 40–46. <https://doi.org/10.1109/RFID.2015.7113071>
- [13] Lhermet, H., Condemine, C., Plissonnier, M., Salot, R., Audebert, P., & Rosset, M. (2008). Efficient Power Management Circuit: From Thermal Energy Harvesting to Above-IC Microbattery Energy Storage. *IEEE Journal of Solid-State Circuits*, 43(1), 246–255. <https://doi.org/10.1109/JSSC.2007.914725>
- [14] Abouzied, M. A., & Sánchez-Sinencio, E. (2015). Low-Input Power-Level CMOS RF Energy-Harvesting Front End. *IEEE Transactions on Microwave Theory and Techniques*, 63(11), 3794–3805. <https://doi.org/10.1109/TMTT.2015.2479233>
- [15] Duong, V., Hieu, N. X., Lee, H., & Lee, J. (2016). A Battery-Assisted Passive EPC Gen-2 RFID Sensor Tag IC With Efficient Battery Power Management and RF Energy Harvesting. *IEEE Transactions on Industrial Electronics*, 63(11), 7112–7123. <https://doi.org/10.1109/TIE.2016.2585463>
- [16] Bito, J., Bahr, R., Hester, J. G., Nauroze, S. A., Georgiadis, A., & Tentzeris, M. M. (2017). A Novel Solar and Electromagnetic Energy Harvesting System With a 3-D Printed Package for Energy Efficient Internet-of-Things Wireless Sensors. *IEEE Transactions on Microwave Theory and Techniques*, 65(5), 1831–1842. <https://doi.org/10.1109/TMTT.2017.2660487>
- [17] Murali, H., Bell, J., Cheng, Q., Mairena, K., Centeno, E., Durgin, G. D., & Shi, E. (2017). Using inkjet printed circuits on a transparent substrate for microwave energy harvesting for space based solar power. *2017 IEEE International Conference on Wireless for Space and Extreme Environments (WiSEE)*, 140–143. <https://doi.org/10.1109/WiSEE.2017.8124907>
- [18] Kim, B. S., Vyas, R., Bito, J., Niotaki, K., Collado, A., Georgiadis, A., & Tentzeris, M. M. (2014). *Ambient RF Energy-Harvesting Technologies for Self-Sustainable Standalone Wireless Sensor Platforms*. 102(11).
- [19] Niotaki, K., Collado, A., Georgiadis, A., Kim, S., & Tentzeris, M. M. (2014). Solar/Electromagnetic Energy Harvesting and Wireless Power Transmission. *Proceedings of the IEEE*, 102(11), 1712–1722. <https://doi.org/10.1109/JPROC.2014.2358646>
- [20] Carvalho, N. B., Georgiadis, A., Costanzo, A., Rogier, H., Collado, A., García, J. A., Lucyszyn, S., Mezzanotte, P., Kracek, J., Masotti, D., Boaventura, A. J. S., de las Nuevas Ruíz Lavín, M., Piñuela, M., Yates, D.C., Mitcheson, P.D., Mazanek, M., & Pankrac, V. (2014). Wireless Power Transmission: R&D Activities Within Europe. *IEEE Transactions on Microwave Theory and Techniques*, 62(4), 1031–1045. <https://doi.org/10.1109/TMTT.2014.2303420>
- [21] Nguyen, S., & Amirtharajah, R. (2018). A hybrid RF and vibration energy

- harvester for wearable devices. *2018 IEEE Applied Power Electronics Conference and Exposition (APEC)*, 1060–1064. <https://doi.org/10.1109/APEC.2018.8341146>
- [22] Kim, S., Bito, J., Jeong, S., Georgiadis, A., & Tentzeris, M. M. (2015). A flexible hybrid printed RF energy harvester utilizing catalyst-based copper printing technologies for far-field RF energy harvesting applications. *2015 IEEE MTT-S International Microwave Symposium*, 1–4. <https://doi.org/10.1109/MWSYM.2015.7166723>
- [23] Bito, J., Hester, J. G., & Tentzeris, M. M. (2017). A fully autonomous ultra-low power hybrid RF/photovoltaic energy harvesting system with -25 dBm sensitivity. *2017 IEEE Wireless Power Transfer Conference (WPTC)*, 1–4. <https://doi.org/10.1109/WPT.2017.7953858>
- [24] Brown, W. C. (1984). The History of Power Transmission by Radio Waves. *IEEE Transactions on Microwave Theory and Techniques*, 32(9), 1230–1242. <https://doi.org/10.1109/TMTT.1984.1132833>
- [25] McSpadden, J. O., Yoo, T., & Chang, K. (1992). Theoretical and experimental investigation of a rectenna element for microwave power transmission. *IEEE Transactions on Microwave Theory and Techniques*, 40(12), 2359–2366. <https://doi.org/10.1109/22.179902>
- [26] Visser, H. J., & Vullers, R. J. M. (2013). RF Energy Harvesting and Transport for Wireless Sensor Network Applications: Principles and Requirements. *Proceedings of the IEEE*, 101(6), 1410–1423. <https://doi.org/10.1109/JPROC.2013.2250891>
- [27] Piñuela, M., Mitcheson, P. D., & Lucyszyn, S. (2013). Ambient RF Energy Harvesting in Urban and Semi-Urban Environments. *IEEE Transactions on Microwave Theory and Techniques*, 61(7), 2715–2726. <https://doi.org/10.1109/TMTT.2013.2262687>
- [28] Scheeler, R., Korhummel, S., & Popovic, Z. (2014). A Dual-Frequency Ultralow-Power Efficient 0.5-g Rectenna. *IEEE Microwave Magazine*, 15(1), 109–114. <https://doi.org/10.1109/MMM.2013.2288836>
- [29] Stoopman, M., Keyrouz, S., Visser, H. J., Philips, K., & Serdijn, W. A. (2014). Co-Design of a CMOS Rectifier and Small Loop Antenna for Highly Sensitive RF Energy Harvesters. *IEEE Journal of Solid-State Circuits*, 49(3), 622–634. <https://doi.org/10.1109/JSSC.2014.2302793>
- [30] Palandöken, M. (2016). Microstrip antenna with compact anti-spiral slot resonator for 2.4 GHz energy harvesting applications. *Microwave and Optical Technology Letters*, 58(6), 1404–1408. <https://doi.org/10.1002/mop.29824>
- [31] Ladan, S., Guntupalli, A. B., & Wu, K. (2014). A High-Efficiency 24 GHz Rectenna Development Towards Millimeter-Wave Energy Harvesting and Wireless Power Transmission. *IEEE Transactions on Circuits and Systems I: Regular Papers*, 61(12), 3358–3366. <https://doi.org/10.1109/TCSI.2014.2338616>
- [32] Kim, S., Vyas, R., Bito, J., Niotaki, K., Collado, A., Georgiadis, A., & Tentzeris,

- M. M. (2014). Ambient RF Energy-Harvesting Technologies for Self-Sustainable Standalone Wireless Sensor Platforms. *Proceedings of the IEEE*, 102(11), 1649–1666. <https://doi.org/10.1109/JPROC.2014.2357031>
- [33] Kanaya, H., Tsukamaoto, S., Hirabaru, T., Kanemoto, D., Pokharel, R. K., & Yoshida, K. (2013). Energy Harvesting Circuit on a One-Sided Directional Flexible Antenna. *IEEE Microwave and Wireless Components Letters*, 23(3), 164–166. <https://doi.org/10.1109/LMWC.2013.2246779>
- [34] Adami, S. E., Proynov, P., Hilton, G. S., Yang, G., Zhang, C., Zhu, D., Li, Y., Beeby, S. P., Craddock, I.J., & Stark, B. H. (2018). A Flexible 2.45-GHz Power Harvesting Wristband with Net System Output from -24.3 dBm of RF Power. *IEEE Transactions on Microwave Theory and Techniques*, 66(1), 380–395. <https://doi.org/10.1109/TMTT.2017.2700299>
- [35] Yang, L., Zhou, Y. J., Zhang, C., Yang, X. M., Yang, X., & Tan, C. (2018). Compact Multiband Wireless Energy Harvesting Based Battery-Free Body Area Networks Sensor for Mobile Healthcare. *IEEE Journal of Electromagnetics, RF and Microwaves in Medicine and Biology*, 2(2), 109–115. <https://doi.org/10.1109/JERM.2018.2817364>
- [36] Sun, H., & Geyi, W. (2017). A New Rectenna Using Beamwidth-Enhanced Antenna Array for RF Power Harvesting Applications. *IEEE Antennas and Wireless Propagation Letters*, 16, 1451–1454. <https://doi.org/10.1109/LAWP.2016.2642124>
- [37] Song, C., Huang, Y., Zhou, J., Zhang, J., Yuan, S., & Carter, P. (2015). A High-Efficiency Broadband Rectenna for Ambient Wireless Energy Harvesting. *IEEE Transactions on Antennas and Propagation*, 63(8), 3486–3495. <https://doi.org/10.1109/TAP.2015.2431719>
- [38] Arrawatia, M., Baghini, M. S., & Kumar, G. (2015). Differential Microstrip Antenna for RF Energy Harvesting. *IEEE Transactions on Antennas and Propagation*, 63(4), 1581–1588. <https://doi.org/10.1109/TAP.2015.2399939>
- [39] Shen, S., Chiu, C., & Murch, R. D. (2017). A Dual-Port Triple-Band L-Probe Microstrip Patch Rectenna for Ambient RF Energy Harvesting. *IEEE Antennas and Wireless Propagation Letters*, 16, 3071–3074. <https://doi.org/10.1109/LAWP.2017.2761397>
- [40] Chuma, E. L., Rodríguez, L. d. l. T., Iano, Y., Roger, L. L. B., & Sanchez-Soriano, M. (2018). Compact rectenna based on a fractal geometry with a high conversion energy efficiency per area. *IET Microwaves, Antennas & Propagation*, 12(2), 173–178. <https://doi.org/10.1049/iet-map.2016.1150>
- [41] Song, C., Huang, Y., Carter, P., Zhou, J., Yuan, S., Xu, Q., & Kod, M. (2016). A Novel Six-Band Dual CP Rectenna Using Improved Impedance Matching Technique for Ambient RF Energy Harvesting. *IEEE Transactions on Antennas and Propagation*, 64(7), 3160–3171. <https://doi.org/10.1109/TAP.2016.2565697>
- [42] Kamoda, H., Kitazawa, S., Kukutsu, N., & Kobayashi, K. (2015). Loop Antenna Over Artificial Magnetic Conductor Surface and Its Application to Dual-Band RF Energy Harvesting. *IEEE Transactions on Antennas and Propagation*,

63(10), 4408–4417. <https://doi.org/10.1109/TAP.2015.2459132>

- [43] Marian, V., Allard, B., Vollaire, C., & Verdier, J. (2012). Strategy for Microwave Energy Harvesting From Ambient Field or a Feeding Source. *IEEE Transactions on Power Electronics*, 27(11), 4481–4491. <https://doi.org/10.1109/TPEL.2012.2185249>
- [44] Ferreira, D., Sismeiro, L., Ferreira, A., Caldeirinha, R. F. S., Fernandes, T. R., & Cuiñas, I. (2016). Hybrid FSS and Rectenna Design for Wireless Power Harvesting. *IEEE Transactions on Antennas and Propagation*, 64(5), 2038–2042. <https://doi.org/10.1109/TAP.2016.2536168>
- [45] Peter, T., Rahman, T. A., Cheung, S. W., Nilavalan, R., Abutarboush, H. F., & Vilches, A. (2014). A Novel Transparent UWB Antenna for Photovoltaic Solar Panel Integration and RF Energy Harvesting. *IEEE Transactions on Antennas and Propagation*, 62(4), 1844–1853. <https://doi.org/10.1109/TAP.2014.2298044>
- [46] Popović, Z., Korhummel, S., Dunbar, S., Scheeler, R., Dolgov, A., Zane, R., Falkenstein, E., & Hagerty, J. (2014). Scalable RF Energy Harvesting. *IEEE Transactions on Microwave Theory and Techniques*, 62(4), 1046–1056. <https://doi.org/10.1109/TMTT.2014.230084>
- [47] Pinuela, M. (2013). Ambient RF Energy Harvesting and Efficient DC-Load Inductive Power Transfer. Imperial College London.
- [48] Alloh, H. M. J. (2016). Design of Rectifier Antenna for Microwave Energy Harvesting Application. The Islamic University.
- [49] Zhang, J. (2013). Rectennas for Rf Wireless Energy Harvesting. The University of Liverpool.
- [50] Sim, Z. W. (2011). Radio Frequency Energy Harvesting for Embedded Sensor Networks in the Natural Environment. The University of Manchester.
- [51] Brynhildsvoll, F. S. (2016). Ambient RF-energy harvesting at 900 MHz. Norwegian University of Science and Technology.
- [52] Mouapi, A., Hakem, N., & Kandil, N. (2017). High efficiency rectifier for RF energy harvesting in the GSM band. *2017 IEEE International Symposium on Antennas and Propagation & USNC/URSI National Radio Science Meeting*, 1617–1618. <https://doi.org/10.1109/APUSNCURSINRSM.2017.8072851>
- [53] Indumathi, G., & Karthika, K. (2015). Rectenna design for RF energy harvesting in wireless sensor networks. *2015 IEEE International Conference on Electrical, Computer and Communication Technologies (ICECCT)*, 1–4. <https://doi.org/10.1109/ICECCT.2015.7226171>
- [54] Ho, D., Kharrat, I., Ngo, V., Vuong, T., Nguyen, Q., & Le, M. (2016). Dual-band rectenna for ambient RF energy harvesting at GSM 900 MHz and 1800 MHz. *2016 IEEE International Conference on Sustainable Energy Technologies (ICSET)*, 306–310. <https://doi.org/10.1109/ICSET.2016.7811800>
- [55] Mansour, M. M., & Kanaya, H. (2018). Compact and Broadband RF Rectifier With 1.5 Octave Bandwidth Based on a Simple Pair of L-Section Matching Network. *IEEE Microwave and Wireless Components Letters*, 28(4), 335–337.

<https://doi.org/10.1109/LMWC.2018.2808419>

- [56] Encyclopedia Britannica. (2013). Radio-frequency spectrum. Retrieved April 1, 2019, from Encyclopædia Britannica website: <https://www.britannica.com/science/radio-frequency-spectrum>
- [57] Balanis, C. A. (2012). *Antenna Theory: Analysis and Design*. Wiley.
- [58] Garg, R. (2001). *Microstrip antenna design handbook*. Boston, Artech House.
- [59] James, J. R., Hall, P. S., & Wood, C. (1986). *Microstrip Antenna: Theory and Design*.
- [60] Kumar, G., & Ray, K. P. (2003). *Broadband Microstrip Antennas*. Artech House.
- [61] Wong, K. L. (2004). *Compact and Broadband Microstrip Antennas*. Wiley.
- [62] Le, T., Mayaram, K., & Fiez, T. (2008). Efficient Far-Field Radio Frequency Energy Harvesting for Passively Powered Sensor Networks. *IEEE Journal of Solid-State Circuits*, 43(5), 1287–1302. <https://doi.org/10.1109/JSSC.2008.920318>
- [63] Abouzied, M. A., Ravichandran, K., & Sánchez-Sinencio, E. (2017). A Fully Integrated Reconfigurable Self-Startup RF Energy-Harvesting System With Storage Capability. *IEEE Journal of Solid-State Circuits*, 52(3), 704–719. <https://doi.org/10.1109/JSSC.2016.2633985>
- [64] Hemour, S., & Wu, K. (2014). Radio-Frequency Rectifier for Electromagnetic Energy Harvesting: Development Path and Future Outlook. *Proceedings of the IEEE*, 102(11), 1667–1691. <https://doi.org/10.1109/JPROC.2014.2358691>
- [65] Shariati, N. (2015). *Sensitive Ambient RF Energy Harvesting*. RMIT University.
- [66] Reinders, A. (2002). Options for photovoltaic solar energy systems in portable products.
- [67] Nintanavongsa, P., Muncuk, U., Lewis, D. R., & Chowdhury, K. R. (2012). Design Optimization and Implementation for RF Energy Harvesting Circuits. *IEEE Journal on Emerging and Selected Topics in Circuits and Systems*, 2(1), 24–33. <https://doi.org/10.1109/JETCAS.2012.2187106>
- [68] Avago Technologies Corp. Designing the Virtual Battery Application Note 1088. Retrieved February 4, 2019, from http://www.hp.woodshot.com/hprfhelpl/4_downld/lit/diodelit/an1088.pdf
- [69] Salter, T., Choi, K., Peckerar, M., Metze, G., & Goldsman, N. (2009). RF energy scavenging system utilising switched capacitor DC-DC converter. *Electronics Letters*, 45(7), 374–376. <https://doi.org/10.1049/el.2009.0153>
- [70] Osman, Z., Azemi, S. N., Ezanuddin, A. A. M., & Kamarudin, L. M. (2016). Compact antenna design for outdoor RF energy harvesting in wireless sensor networks. *2016 3rd International Conference on Electronic Design (ICED)*, 199–202. <https://doi.org/10.1109/ICED.2016.7804636>
- [71] Arrawatia, M., Baghini, M. S., & Kumar, G. (2011). RF energy harvesting system from cell towers in 900MHz band. *2011 National Conference on Communications (NCC)*, 1–5. <https://doi.org/10.1109/NCC.2011.5734733>

- [72] Tavares, J., Barroca, N., Saraiva, H. M., Borges, L. M., Velez, F. J., Loss, C., Salvado, R., Pinho, P., Goncalves, R., & Carvalho, N. B. (2013). Spectrum opportunities for electromagnetic energy harvesting from 350 MHz to 3 GHz. *2013 7th International Symposium on Medical Information and Communication Technology (ISMICT)*, 126–130. <https://doi.org/10.1109/ISMICT.2013.6521714>
- [73] Taris, T., Vigneras, V., & Fadel, L. (2012). A 900MHz RF energy harvesting module. *10th IEEE International NEWCAS Conference*, 445–448. <https://doi.org/10.1109/NEWCAS.2012.6329052>
- [74] Zakaria, Z., Zainuddin, N. A., Aziz, M. Z. A. A., Husain, M. N., & Mutalib, M. A. (2013). Dual-band monopole antenna for energy harvesting system. *2013 IEEE Symposium on Wireless Technology & Applications (ISWTA)*, 225–229. <https://doi.org/10.1109/ISWTA.2013.6688775>
- [75] AbdelTawab, A. M., & Khattab, A. (2016). Efficient multi-band energy Harvesting circuit for Wireless Sensor Nodes. *2016 Fourth International Japan-Egypt Conference on Electronics, Communications and Computers (JEC-ECC)*, 75–78. <https://doi.org/10.1109/JEC-ECC.2016.7518971>
- [76] Song, C., Huang, Y., Zhou, J., Carter, P., Yuan, S., Xu, Q., & Fei, Z. (2017). Matching Network Elimination in Broadband Rectennas for High-Efficiency Wireless Power Transfer and Energy Harvesting. *IEEE Transactions on Industrial Electronics*, 64(5), 3950–3961. <https://doi.org/10.1109/TIE.2016.2645505>
- [77] Palazzi, V., Prete, M. Del, & Fantuzzi, M. (2017). Scavenging for Energy: A Rectenna Design for Wireless Energy Harvesting in UHF Mobile Telephony Bands. *IEEE Microwave Magazine*, 18(1), 91–99. <https://doi.org/10.1109/MMM.2016.2616189>
- [78] Sun, H., Guo, Y., He, M., & Zhong, Z. (2013). A Dual-Band Rectenna Using Broadband Yagi Antenna Array for Ambient RF Power Harvesting. *IEEE Antennas and Wireless Propagation Letters*, 12, 918–921. <https://doi.org/10.1109/LAWP.2013.2272873>
- [79] Agarwal, K., Mishra, T., Karim, M. F., Nasimuddin, Chuen, M. O. L., Guo, Y. X., & Panda, S. K. (2013). Highly efficient wireless energy harvesting system using metamaterial based compact CP antenna. *2013 IEEE MTT-S International Microwave Symposium Digest (MTT)*, 1–4. <https://doi.org/10.1109/MWSYM.2013.6697693>
- [80] Adami, S., Zhu, D., Li, Y., Mellios, E., Stark, B. H., & Beeby, S. (2015). A 2.45 GHz rectenna screen-printed on polycotton for on-body RF power transfer and harvesting. *2015 IEEE Wireless Power Transfer Conference (WPTC)*, 1–4. <https://doi.org/10.1109/WPT.2015.7140161>
- [81] Mishra, T., Panda, S. K., Karim, M. F., Ong, L. C., & Chiam, T. M. (2012). 2.4GHz square slot antenna and power management circuit for wireless energy harvesting applications. *2012 IEEE Asia-Pacific Conference on Antennas and Propagation*, 223–224. <https://doi.org/10.1109/APCAP.2012.6333227>
- [82] Ahmed, S., Zakaria, Z., Husain, M. N., & Alhegazi, A. (2017). Integrated

- rectifying circuit and antenna design with harmonic rejection for RF energy harvesting. *2017 11th European Conference on Antennas and Propagation (EUCAP)*, 1940–1944. <https://doi.org/10.23919/EuCAP.2017.7928106>
- [83] Wen, J., Xie, D., Liu, X., Guo, H., Liu, C., & Yang, X. (2016). Wideband collar-shaped antenna for RF energy harvesting. *2016 Asia-Pacific International Symposium on Electromagnetic Compatibility (APEMC), 01*, 253–255. <https://doi.org/10.1109/APEMC.2016.7523025>
- [84] Gudan, K., Shao, S., Hull, J. J., Hoang, A., Ensworth, J., & Reynolds, M. S. (2015). Ultra-low power autonomous 2.4GHz RF energy harvesting and storage system. *2015 IEEE International Conference on RFID Technology and Applications (RFID-TA)*, 176–181. <https://doi.org/10.1109/RFID-TA.2015.7379814>
- [85] KY-028 Digital Temperature Sensor Module. (2017). KY-028 Datasheet. Retrieved March 10, 2019, from Arduino Modules website: [http://sensorkit.en.joy-it.net/index.php?title=KY-028_Temperature_Sensor_module_\(Thermistor\)](http://sensorkit.en.joy-it.net/index.php?title=KY-028_Temperature_Sensor_module_(Thermistor))
- [86] Computer Simulation Technology. (2019). CST Studio Suite. Retrieved July 5, 2018, from <https://www.cst.com/products/csts2>
- [87] Rogers Corporation. (2018). RO4003C™ Laminates. Retrieved June 7, 2018, from <https://www.rogerscorp.com/acs/products/54/RO4003C-Laminates.aspx>
- [88] Skyworks Inc. (2015). SMS7630-061 Datasheet. Retrieved May 10, 2019, from http://www.skyworksinc.com/uploads/documents/SMS7630_061_201295H.pdf
- [89] Ansys Electromagnetics. (2016). Ansys Electronics Desktop. Retrieved November 17, 2018, from <https://www.ansys.com/products/electronics>

CURRICULUM VITAE



Name Surname : Cem GÖÇEN
Place and Date of Birth : Izmir, 1992
Adress : Izmir Katip Çelebi University, Balatçık, Çiğli, Izmir
E-mail : gocencem@gmail.com, cem.gocen@ikc.edu.tr
Work Experience : Research Assistant (Izmir Katip Çelebi University, 2019 - ...)

Education:

B. Sc.: 2016, Ankara University, Department of Electrical - Electronics Engineering

List of Publications:

Conference Papers

1. Baytöre, C., Zoral, E. Y., **Göçen, C.**, Palandöken, M., & Kaya, A. (2018). Coplanar flexible antenna design using conductive silver nano ink on paper substrate for wearable antenna applications. *2018 28th International Conference Radioelektronika, RADIOELEKTRONIKA 2018*, 1–6. <https://doi.org/10.1109/RADIOELEK.2018.8376382>

2. **Göçen, C.**, Palandöken, M., & Kaya, A. (2018). A Novel Compact Microstrip Antenna for GSM900 Band RF Energy Harvesting Applications. *6th Eur. Conf. Ren. Energy Sys. 25-27 June 2018, Istanbul, Turkey.*
3. **Göçen, C.**, Palandöken, M., & Kaya, A. (2018). ISM Bandı RF Enerji Hasatlama Uygulamaları için Metamalzeme Yapılarından Esinlenen Yeni Mikroşerit Anten Tasarımı. *IX. URSI-70. ULTRATHIN WAVELENGTH MICROSTRUCTURED ANTENNAS FOR WIRELESS ENERGY HARVESTING APPLICATIONS*. - (00) .

SCI Journal Papers

1. Palandoken, M., **Gocen, C.**, Kaya, A., Gunes, F., Baytore, C., & Can, F. C. (2018). A novel split-ring resonator and voltage multiplier based rectenna design for 900 MHz energy harvesting applications. *Radioengineering*, 27(3), 711–717. <https://doi.org/10.13164/re.2018.0711>
2. Palandoken, M., & **Gocen, C.** (2019). A modified Hilbert fractal resonator based rectenna design for GSM900 band RF energy harvesting applications. *International Journal of RF and Microwave Computer-Aided Engineering*, 29(1). <https://doi.org/10.1002/mmce.21643>
3. Kaur, K. P., Upadhyaya, T., Palandoken, M., & **Gocen, C.** (2019). Ultrathin dual-layer triple-band flexible microwave metamaterial absorber for energy harvesting applications. *International Journal of RF and Microwave Computer-Aided Engineering*, 29(1). <https://doi.org/10.1002/mmce.21646>
4. Desai, A., Upadhyaya, T., Palandoken, M., & **Gocen, C.** (2019). Dual band transparent antenna for wireless MIMO system applications. *Microwave and Optical Technology Letters*, 61(7), 1845–1856. <https://doi.org/10.1002/mop.31825>